2020

ASSESSING THE CLIMATE WATER BALANCE MODEL'S ABILITY TO PREDICT SOIL MOISTURE VARIABILITY AND SPECIES DISTRIBUTION OF A FORESTED WATERSHED IN THE NORTHERN CUMBERLAND PLATEAU

Katherine J. Love
University of Kentucky, katherine.love@uky.edu
Digital Object Identifier: https://doi.org/10.13023/etd.2020.276

STUDENT AGREEMENT:

I represent that my thesis or dissertation and abstract are my original work. Proper attribution has been given to all outside sources. I understand that I am solely responsible for obtaining any needed copyright permissions. I have obtained needed written permission statement(s) from the owner(s) of each third-party copyrighted matter to be included in my work, allowing electronic distribution (if such use is not permitted by the fair use doctrine) which will be submitted to UKnowledge as Additional File.

I hereby grant to The University of Kentucky and its agents the irrevocable, non-exclusive, and royalty-free license to archive and make accessible my work in whole or in part in all forms of media, now or hereafter known. I agree that the document mentioned above may be made available immediately for worldwide access unless an embargo applies.

I retain all other ownership rights to the copyright of my work. I also retain the right to use in future works (such as articles or books) all or part of my work. I understand that I am free to register the copyright to my work.

REVIEW, APPROVAL AND ACCEPTANCE

The document mentioned above has been reviewed and accepted by the student's advisor, on behalf of the advisory committee, and by the Director of Graduate Studies (DGS), on behalf of the program; we verify that this is the final, approved version of the student's thesis including all changes required by the advisory committee. The undersigned agree to abide by the statements above.

Katherine J. Love, Student

Dr. Jian Yang, Major Professor

Dr. Steven J. Price, Director of Graduate Studies

ASSESSING THE CLIMATE WATER BALANCE MODEL'S ABILITY TO PREDICT SOIL MOISTURE VARIABILITY AND SPECIES DISTRIBUTION OF A FORESTED WATERSHED IN THE NORTHERN CUMBERLAND PLATEAU

THESIS

A thesis submitted in partial fulfillment of the
requirements for the degree of Master of Science in Forest and Natural Resource Sciences in the College of Agriculture, Food and Environment
at the University of Kentucky

By
Katherine J. Love
Lexington, Kentucky
Co-Directors: Dr. Jian Yang, Assistant Professor of Forest Landscape Ecology
and Dr. John Lhotka, Associate Professor of Silviculture
Lexington, Kentucky
2020

ABSTRACT OF THESIS

ASSESSING THE CLIMATE WATER BALANCE MODEL'S ABILITY TO PREDICT SOIL MOISTURE VARIABILITY AND SPECIES DISTRIBUTION OF A FORESTED WATERSHED IN THE NORTHERN CUMBERLAND PLATEAU

Spatial patterns of moisture and tree species have been studied using environmental gradients, often represented by terrain attributes in GIS. With climate change, GIS terrain variables, which are static as long as the elevation remains unchanged, will not reflect alterations in temperature, water cycle, and atmospheric conditions. In this thesis, the commonly used terrain variables and climate water balance variables were evaluated and compared for their ability to explain soil moisture and tree species distributions in a forested watershed in the Northern Cumberland Plateau. The results suggest that GIS terrain variables generally perform better than climate water balance variables, however, the differences are not significant for soil moisture or half of the species studied. Topographic position, a terrain attribute not explicitly considered by climate water balance variables, performed well in its ability to explain both soil moisture and tree species distributions. This suggests that the inclusion of topographic position into or in tandem with future iterations of climate water balance variables could be advantageous.

KEYWORDS: Terrain Analysis, Climate Water Balance, Soil Moisture, Tree Distributions

Katherine J. Love

6/17/2020

ASSESSING THE CLIMATE WATER BALANCE MODEL'S ABILITY TO PREDICT SOIL MOISTURE VARIABILITY AND SPECIES DISTRIBUTION OF A FORESTED WATERSHED IN THE NORTHERN CUMBERLAND PLATEAU

By
Katherine J. Love

Dr. Jian Yang
Co-Director of Thesis

Dr. John Lhotka
Co-Director of Thesis

Dr. Steven Price
Director of Graduate Studies

6/17/2020

DEDICATION

To my grandparents, Verna Jean, James, Nancy, and Jon, whose hard work paved the way. And especially to my parents, Jim and Sue, for everything.

ACKNOWLEDGEMENTS

There are many people who supported this work in various ways. I would like to thank my co-advisors, Dr. Jian Yang and Dr. John Lhotka, and committee member, Dr. Chris Barton, for their advice and insight throughout this process. Thank you to the University of Kentucky Department of Forestry and Natural Resources and the University of Kentucky Appalachian Center for financially supporting me and the research of this project. I would also like to thank those who so generously helped with fieldwork, bringing optimism, humor, and endless determination along with them, including Dan Eaton, Brandon Foley, and Alex Murphie, Jena Nierman, and Kamana Poudel. Thank you to Zach Hackworth who helped with each component of fieldwork and for his help with statistical analysis. Thank you to the staff at Robinson Forest, especially David Collett, Neva Williams, and Erwin Williams, for their assistance and hospitality. To my graduate student cohort for creating a supportive community.

A special thanks to my family, especially Matt, Brie, and my parents, for their unwavering love, patience, and optimism. And lastly, to Thomas for his love and encouragement, as well as his help with fieldwork and shared experience throughout our graduate programs.

TABLE OF CONTENTS

LIST OF TABLES

LIST OF FIGURES

CHAPTER 1 INTRODUCTION

Highly variable topography creates heterogeneous microclimates, vegetation, and soil properties, which have been a focus of ecological studies over the past century. Climate change presents a force of disturbance that affects vegetation phenology (Bertin 2008; Cleland et al. 2007; Doi and Katano 2008), productivity (Boisvenue and Running 2006), mortality (Allen et al. 2010; McDowell and Allen 2015), and spatial distribution (Davis and Shaw 2001; Kelly and Goulden 2008). Dissected landscapes present unique systems to study how climate change will affect vegetation distributions, due in part to the complex range of site conditions.

In the forests of the Eastern United States, early ecologists identified plant community composition within variable landscapes and identified how they changed in relation to aspect, topographic position, and subsequently, moisture gradients (Braun 1950; Whittaker 1967). In Kentucky and Tennessee, the influences of aspect and topographic position on distributions of soil moisture and soil properties are well documented, in addition to their relationship with tree species distribution (Fralish et al. 1993; Franklin et al. 1993). Ridges, upper slope positions, and southwest-facing slopes are typically characterized by lower soil moisture and soil nutrients compared to lower slope positions and northeast-facing slopes. Oaks (*Quercus* spp.) and hickories (*Carya* spp.) are found in the xeric, upper slope and ridge sites. American beech (*Fagus grandifolia*), sugar maple (*Acer saccharum*), and tulip poplar (*Liriodendron tulipifera*) are found at mesic sites, which are often northeast-facing or at lower topographic positions. Available water capacity, slope position, soil pH, elevation, and percent rock

were found to explain tree species distributions in western Kentucky and Tennessee (Fralish et al. 1993; Franklin et al. 1993).

With technological advances, environmental gradients can be easily derived using Geographic Information Systems (GIS). While field observations are still necessary, terrain data that would have required field visits can now be calculated remotely at higher resolutions with few data inputs. Terrain variables representing patterns of aspect, elevation, solar radiation, soil moisture, and topographic position can be calculated for a given study area using GIS and a Digital Elevation Model (DEM). Although GIS-derived terrain variables may be able to capture or be correlated with plant relevant resources, they are static variables that will not change over time, a disadvantage when considering how changing climate will affect the spatial and temporal distributions of plant resources.

The climate water balance (CWB) is a concept that represents the simultaneous availability of water and energy as experienced by plants. This allows ecologists to consider annual and monthly water balance at a site, instead of metrics that reflect annual totals such as potential evapotranspiration and precipitation. The CWB concept is implemented as a suite of GIS variables produced by the Water Balance Toolset 3.0.2 (Dyer 2009). The CWB toolset equips users with the ability to calculate CWB for their study area using monthly climate, solar radiation, and soil data while considering how the topography of the area alters the spatial distribution of these elements. The integration of fine-scale terrain data with temporally dynamic climate data enables the toolset to capture differences in solar radiation, evapotranspiration, and water availability throughout a landscape. A dynamic GIS variable that represents the balance of water, influenced by

available energy and water, presents benefits when studying vegetation distribution, especially under changing climate conditions.

Dyer (2009, 2019) studied the ability of this CWB toolset to explain soil moisture and tree species distribution in the Eastern United States. Though these studies found CWB toolset variables correlated with soil moisture (Dyer 2009) and corresponding with tree distribution (Dyer 2019), an in-depth evaluation of the toolset is needed. The current toolset does not take into account topographic position in the calculation of water availability. In dissected landscapes, topography is associated with many ecological patterns, including soil chemistry, vegetation composition, and forest productivity due to the movement of water and nutrients to lower slope positions (Fisher and Binkley 2000). An assessment of the CWB toolset in representing soil moisture patterns and vegetation distributions in the Cumberland Plateau can better inform how GIS is used to represent these ecological patterns. There are two overarching objectives of this thesis: 1. to assess the ability of the current climate water balance GIS toolset to represent soil moisture variability at fine spatial resolutions and 2. to assess how well tree species distributions in a dissected landscape are explained by the current climate water balance GIS toolset.

CHAPTER 2 ASSESSING THE REPRESENTATION OF SOIL MOISTURE

INTRODUCTION

Estimating the water available to plants is an increasingly important issue under changing climate scenarios. Plant water availability and microclimate influence species composition (Stephenson 1998), species distribution (Whittaker 1956), productivity (Whittaker 1966), soil formation (Jenny 1980), and forest flammability (Clark 1990; Miller and Urban 1999). Climate change will result in alterations of temperature, water cycle, atmospheric conditions, and energy budget (Collins et al. 2013). As these changes can influence precipitation patterns and evaporative demand, plant water availability should be at the forefront when considering how plants adapt to shifting climate circumstances (Crimmins et al. 2011; Lenoir et al. 2017; McLaughlin et al. 2017; VanDerWal et al. 2013). Terrain variables created using Geographic Information Systems (GIS) have shown to represent static patterns of soil moisture, however, under changing climate circumstances, the use of dynamic GIS variables that reflect site-specific simultaneous availability of water and energy can be advantageous (Stephenson 1990). An investigation into how spatial variables derived using GIS represent soil moisture patterns in dissected landscapes is needed. In this study, the ability of commonly used terrain and water balance GIS variables to represent soil moisture is investigated.

In studying plant available water, many factors need to be considered including climate, soil attributes such as texture, topography, and plant specific attributes such as rooting zones. Estimating how much water is available to a plant during a given time is difficult due to the complex interaction of influential factors, however, soil moisture is often used as a surrogate for understanding what the patterns of moisture are in the field.

Topography of heterogeneous landscapes can create varied microclimate, soil properties, and vegetation patterns (Boerner 2006). Three topographic gradients that are used to study the heterogeneity of these landscapes are slope aspect, topographic position, and slope curvature.

Dissected landscapes, such as in the Appalachian region of the Eastern United States, have been the focus of many ecological studies due to influences of the complex terrain on ecological patterns and processes. For example, it has been documented that adjacent northeast and southwest aspects in the Cumberland Plateau of the Appalachian region have different air temperature, soil temperature, soil moisture, relative humidity, soil nutrients, and vegetation (Hutchins et al. 1976). Northeast-facing slopes often have higher pH values, soil nutrients, soil moisture, and mesic species, while opposing southwest-facing slopes experience more exposure to solar radiation and support species adapted to xeric site conditions with lower soil pH and water holding capacity (Hutchins et al. 1976). Topography can affect drainage patterns (Beven and Kirkby 1979), exposure to solar radiation (Franzmeier et al. 1969), as well as soil properties and erosion (Moore et al. 1993). Valley positions, though on adjacent aspects, may experience similar levels of solar radiation due to the shading effects of the surrounding topography. These sheltering effects result in cooler air temperatures and increased moisture (Franzmeier et al. 1969). Hydrologic flow is mediated by topography as gravity moves water downslope (Beven and Kirkby 1979; Lookingbill and Urban 2004).

The distribution of trees along topographic gradients is evident in the Eastern United States (Braun 1942; Whittaker 1956). In the Great Smoky Mountains, Whittaker (1956) described forest communities along elevation, topographic position, and moisture

gradients. Ridges, peaks, and open slopes were characterized as xeric sites, while coves, canyons, flats, ravines, and sheltered slopes were characterized as mesic (Whittaker 1956). In the Cumberland Mountains, Braun (1942) noted species distributions along elevation and topographic position gradients. Day and Monk (1974) studied tree distributions in North Carolina with relation to elevation, aspect, distance from stream channel, and distance from the water divide. They noted that soil moisture was the most important environmental gradient corresponding with the topographic elements they studied (Day and Monk 1974). In western Kentucky and Tennessee, the distribution of species and communities along moisture gradients is evident (Fralish et al. 1993; Franklin et al. 1993). Xeric sites in the Kentucky and Tennessee region are associated with oak (*Quercus* spp.) and hickory (*Carya* spp.), while the mesic sites are associated with beech (*Fagus grandifolia*), sugar maple (*Acer saccharum*), magnolia (*Magnolia* spp.), and tulip poplar (*Liriodendron tulipifera*) (Fralish et al. 1993; Franklin et al. 1993). In southeastern Kentucky similar patterns are identified, including *Fagus grandifolia* at lower slope positions and *Quercus prinus* (= *Quercus montana*) and *Acer rubrum* at upper slope positions (Muller 1982). In North Carolina, similar distributions were found, with *Quercus montana* positively correlated with elevation (Day and Monk 1974).

To capture the complex influence of terrain on the ecology of an area, GIS-derived variables have been produced to represent ecological processes, such as the spatial distribution of moisture in landscapes. Two popular moisture indices include the topographic wetness index (TWI) and the integrative moisture index (IMI). TWI quantifies the control topography has on hydrologic flow by considering the upslope contributing area of a given point and the slope of the surrounding area (Beven and

Kirkby 1979). IMI accounts for solar radiation, flow accumulation, slope curvature, and soil total water capacity (Iverson et al. 1997). These moisture indices have been shown to represent patterns of soil moisture (Iverson et al. 2004a; Sørensen et al. 2006), however, these variables are temporally static and are relative measurements of moisture which cannot be compared across sites (Dyer 2009).

As temperature and precipitation trends change throughout the year in many areas of the world, static moisture gradients do not fully explain the availability of water in terms of what is ecologically available. Furthermore, climate change presents scenarios where the interannual patterns of temperature and precipitation will change in both timing and amount. To better understand climate conditions and the influences of topography on the distribution of resources, such as moisture, temporally dynamic spatial variables should be implemented.

Climate Water Balance

The climate water balance (CWB), which has gained popularity in ecology, considers the simultaneous availability of energy and water (Stephenson 1990). CWB reaches beyond the traditional approach of measuring annual energy and water supply and addresses the need to calculate the monthly and annual balance of water as experienced by plants.

CWB incorporates many aspects of the study area, including the available water and rates of evapotranspiration. The available water is water that the plants can uptake which considers the water holding capacity of the soil. The ability of soil to hold water varies across soil types, therefore, considering soil properties in water balance calculations is crucial. For calculating available energy, potential evapotranspiration

(PET) is used, which is the rate at which evapotranspiration would occur when water is not a limiting factor (Rosenberg et al. 1983). Many calculations of evapotranspiration use a standard crop to calculate this rate, though this rate is the same across vegetation types (Monteith 1965; Stephenson 1990; Thom 1975). PET is influenced by the amount of energy available and can be quantified by using temperature, solar radiation, humidity, and wind speed data (Jensen and Allen 2016). The actual evapotranspiration (AET) is the rate of evapotranspiration as experienced by plants, which considers the water and energy biologically available at the site (Major 1963; Rosenzweig 1968). When the water available to the plant does not meet the evaporative demand, the actual evapotranspiration rate is less than the potential evapotranspiration rate, causing a deficit. Conversely, when the available water is more than what is needed to fulfill the evaporative demand of potential evapotranspiration, there is a water surplus (Stephenson 1990).

The balance of water and energy, as well as their timing throughout the year, can enable ecologists to better understand and spatially represent ecological processes. Plant species have varying levels of water needs and deficit thresholds, therefore these CWB variables have been shown to differ between biomes (Stephenson 1990) and tree species (Lutz et al. 2010). CWB metrics have also been shown to be correlated with net primary production (Lieth 1975; Rosenzweig 1968), tree species richness (Currie 1991; Currie and Paquin 1987), and litter decomposition rates (Berg et al. 1993; Dyer et al. 1990; Meentemeyer 1978).

GIS Climate Water Balance

As technology and spatial data become more readily available, conceptual models such as CWB can utilize GIS to approximate CWB metrics using climate, soil, and terrain data. The progression of technology has made fine resolution terrain data available for many locations, such as Light Detection and Ranging (LiDAR)-derived digital elevation models (DEMs). Dyer (2009) developed an ArcGIS toolset that allows users to calculated CWB metrics for their study area with few user inputs. The CWB toolset incorporates both the simultaneous availability of water and energy, as well as how the topography modifies the distribution of these climate variables. The toolset produces many output rasters for the given study area including monthly and annual PET, AET, deficit, moisture storage, and moisture surplus (Dyer 2009).

To run the CWB toolset in ArcGIS, data inputs including a DEM of the study area, soil available water capacity (AWC), monthly precipitation, temperature, and solar radiation are needed (Dyer 2009). The user can either supply this data or download it from publicly available databases, which can be automated by the toolset. National Resources Conservation Service (NRCS 2019) and PRISM Climate data (PRISM Climate Group 2019) provide soil and climate data for the United States. With this input data, this toolset uses the Thornwaite approach (Mather 1978) to calculate components of the hydrologic cycle and the Turc equation to calculate PET (Turc 1961). The Turc equation incorporates both air temperature and solar radiation when calculating PET, which allows this toolset to reflect the role of topography in modifying energy available to a site (Dyer 2019).

The ability of the CWB toolset to represent moisture demand and moisture availability at fine scales, such as within a landscape, can be impacted by its ability to

capture the landform processes. Dyer (2009) studied the capacity of the model to account for variability in soil moisture by using soil moisture sensors at two study areas, one of steep relief in North Carolina and one with moderate relief in Ohio. Though this study validated the toolset's ability to differentiate between aspects and general topographic positions, the ability of the current CWB toolset to characterize the spatial variability of soil moisture at fine spatial resolutions was not addressed. Chiefly, terrain modifies hydrologic and erosion processes (Moore et al. 1993), including runoff, soil water content, and sedimentation, which are not fully considered by the GIS CWB toolset.

The distribution of moisture throughout a landscape is subject to many processes, which makes it difficult to capture spatial patterns with one variable. Understanding the role that topography plays in mediating soil moisture in landscapes permits a better synthesis for quantifying plant available water. Additionally, investigating the ability of commonly used GIS terrain variables and variables produced by the CWB toolset to represent soil moisture variability will inform decisions on how GIS is used to represent ecological processes and patterns. Representing the spatial variability of soil moisture will be crucial in determining how water availability and deficit are considered in models that inform plant distribution patterns. The overarching objective of this study was to assess the current CWB model's ability to represent soil moisture variability at fine spatial resolutions in a highly dissected landscape of central Appalachia. There are three objectives: 1. to quantify the relative role of terrain attributes, including slope aspect, topographic position, and slope curvature, in regulating soil moisture variability, 2. to assess and compare the explanatory power of commonly used GIS terrain and CWB variables in explaining soil moisture, and 3. to evaluate the performance of models with

terrain variables, CWB variables, and the combination of terrain and CWB variables in representing field measured soil moisture.

METHODS

Study Area

The study area is Little Millseat watershed in the Cumberland Plateau and the Appalachian Coalfields of southeastern Kentucky. Little Millseat watershed, a subwatershed of Clemons Fork watershed, is situated in the University of Kentucky's Robinson Forest, a temperature deciduous broadleaf forest spanning 6,000 hectares. Robinson Forest is characterized by steep slopes and soils developed through residuum or colluvium (Hutchins et al. 1976; Williamson et al. 2015). The underlying parent material is from the Breathitt Formation of Pennsylvanian age and consists of sandstone, shale, and siltstone (Hutchins et al. 1976; Hinrichs 1978; McDowell 1985). The 0 to 45-degree slopes of Little Millseat watershed are predominantly northeast and southwest-facing. Due to the dissected nature of this study area, the differences in soil and vegetation between adjacent slopes in Robinson Forest have been studied previously (Abnee et al. 2004; Cremeans 1992; Hutchins et al. 1976; Kalisz 1986).

In the 1800s, some of the dissected slopes in what is now Robinson Forest were cleared for agriculture, later succeeding back to forest. Known as "old fields", slopes that were used for growing crops have noticeable differences in soil characteristics, such as increased rock material (Kalisz 1986). Little Millseat watershed does not have evidence of old fields which would influence the spatial patterns of soil properties.

Experiment Design

Plot locations were determined using a three-way factorial design, with factors including aspect, topographic position, and slope curvature (Figure 2.1). Two aspects (northeast and southwest), five topographic positions (ridge, upper slope, middle slope,

lower slope, and valley), and two slope curvatures (convex and concave) were considered. These strata were chosen due to their role in influencing soil moisture and soil attributes. With this sampling design, there are 20 unique combinations, which were replicated five times, resulting in 100 study plots.

GIS was used to derive the locations of the plots before going into the field. The middle section of Little Millseat watershed has predominantly northeast and southwest-facing slopes. Slope curvature was determined by viewing Topographic Wetness Index (TWI) and hillshade maps which were derived from a 1.5-meter LiDAR-derived DEM. The topographic position classes were determined using the Topography Toolbox for ArcGIS (Dilts 2015). A circular neighborhood with a 100-cell search radius was used to create the Topographic Position Index (TPI) raster, which was then displayed as five topographic positions (ridge, upper slope, middle slope, lower slope, and valley). The 100-cell radius search radius was selected after other search radii of equal or less value produced with less spatially contiguous class distinctions.

After reviewing TWI and hillshade maps for the study area, transects were created in ArcMap along the concave and convex features, with five convex/five concave transects on the northeast-facing slope and five convex/five concave transects on the southwest-facing slope. The TPI output was then imported into ArcMap with the overlaid transects. Five plot centers were then placed along each transect, one per topographic position. For the ridge class, plots were placed at the uppermost part of the ridge, while the remaining classes were placed systematically in the center of the TPI range for that class. Plots were moved in ArcMap if they were within 11 meters of any forest access road, as to avoid the effects the roads may have on hydrology or disturbance history. This

provided the largest plots approximately three meters of space between the outermost edge of the plot and the road. These changes were done to reduce the impacts of the road from disturbance and drainage perspectives. Coordinates derived from these maps were then exported to Avenza Maps and used to navigate during fieldwork (Avenza Systems, Inc. Toronto, ON, Canada).

The plots were established in early May 2019, the plot centers were marked using fiberglass stakes, flagging, and metal numbered tags. For plots on ridge top positions, disturbance effects from mining or forestry operations in the adjacent watersheds (increased stem density and invasive species) prompted the relocation of some plots to about nine meters downslope (while remaining in the ridge TPI class). The coordinates of the established plot centers were recorded using a SXBlue II GNSS GPS receiver (Geneq, Inc., Montreal, QC, Canada). XY accuracy for 99% of the plots was under two meters, one plot had three-meter accuracy. The coordinates were imported into ArcGIS in the WGS 1984 (G1150) coordinate system, then projected to NAD 1983 StatePlane Kentucky FIPS 1600 Feet.

Soil Sampling

Soil samples were collected over the course of four trips in July 2019. One composite soil sample was collected from each of the 100 plots by taking three soil samples collected using a Sharpshooter shovel and mixing them in a plastic bucket. The depth of the O horizon of each soil sample was recorded and the discarded, as the O horizon was not included in the composite sample. Samples were approximately ten centimeters in depth, not including the O horizon. The samples were randomly distributed

within 1.8 meters of the plot center. The bucket used in the mixing process was then brushed out between each composite sample to reduce contamination.

Each composite soil sample was placed in a resealable plastic bag and double bagged to reduce moisture loss during transport since Gravimetric Water Content (GWC) measurements were taken. Soil samples were transported to the lab, transferred into paper bags, and air-dried. Regulatory Services at the University of Kentucky processed the samples. A routine soil test was performed including: 1 M KCl soil pH, Sikora II Buffer pH, Mehlich III calcium (Ca), magnesium (Mg), zinc (Zn), phosphorus (P), and potassium (K). Additional tests were performed including texture class via micropipette method (Burt et al. 1993; Miller and Miller 1987), total carbon, total nitrogen, and water holding potential (percent water at field capacity, percent water at the wilting point, percent plant available water held between field capacity and the wilting point) (Topp et al. 1993).

Soil Moisture Sampling

Onset's 10HS Soil Moisture Smart Sensors and HOBO Micro Station Data Loggers were used to monitor temporal dynamics of soil moisture (Onset Computer Corporation, Bourne, MA, USA); 20 of the 100 plots had these continuous monitoring systems installed. A random number generator was used to select a transect to represent each of the four combinations (northeast concave, northeast convex, southwest concave, southwest convex). The selected transects then had five stations installed, one at each of the five topographic positions studied (ridge, upper slope, middle slope, lower slope, and valley).

The Micro Station systems were installed in late May/early June 2019 at the center of each of the 20 selected plots. Per instructions provided by Onset, to install the 10HS Soil Moisture Smart Sensors a small hole was dug to ten centimeters. A soil knife was then used to make a pilot hole, as rocks and other objects risk harming the sensor. The sensor was then inserted vertically into the pilot hole. The HOBO Micro Station Data Loggers were secured to T posts and the sensor wire was fed through a PVC pipe to protect against damage. A lateral space of .3 meters or more on the ground was created between the sensor and the T post to prevent the presence of metal altering the sensor's reading. Each Micro Station deployed to record the volumetric water content every ten minutes from early June to November 2019.

For all 100 plots, volumetric water content was measured instantaneously using Spectrum Technologies, Inc.'s FieldScout TDR 300 Soil Moisture Meter with 20-centimeter rods (Spectrum Technologies Inc., Aurora, IL, USA). Five readings were randomly taken per plot, within an eight-meter radius of the plot center. The random nature was due to the occurrence of trees and rocks which prevented a systematic sampling design. The time domain reflectometry (TDR) readings for each plot were taken throughout July and the first week of August. The sampling of all 100 plots did not occur during a continuous sampling period, therefore differences in precipitation amounts and weather experienced among the five collections trips should be noted. At the time the TDR measurements were taken, GWC samples were collected for each plot, except for eight plots due to a malfunction with the TDR instrument, which were collected at a later date.

GWC measurements were calculated using a subsample from the composite soil samples. Within the same day of soil collection, each sample was double bagged to reduce moisture loss. The samples were then processed within two days of returning from the collection trip and within three days of collecting the sample in the field. Once in the lab, 50 grams of wet soil was weighed out and placed in pre-weighed aluminum foil boats. The samples were placed in the oven at 110°C for 24 hours. Each sample was then placed in a desiccator for 15 minutes while the soil cooled to room temperature. Each sample's dry weight was recorded. Using the weights of the wet soil, dry soil, and tin, the GWC was calculated for each composite soil sample.

Predictor Variables

Two GIS software programs, ESRI ArcGIS for Desktop 10.6 (ESRI 2011) and SAGA GIS (Conrad et al. 2015), were used to calculate the predictor variable rasters, all of which were derived from a 1.5-m LiDAR-derived DEM. Slope steepness and solar radiation were calculated with ArcGIS for Desktop, topographic wetness index (TWI), relative slope position (RSP), aspect (used to calculate southwestness), and plan curvature were calculated with SAGA GIS. CWB metrics, including storage, surplus, PET, and deficit, were calculated using the Water Balance Toolset version 3.0.2 (Dyer 2009) in ArcGIS for Desktop 10.6. For each of the rasters used in this study, the values for each of the 100 plots were extracted with no focal mean. The boundary of Little Millseat was delineated in ArcGIS and used in clipping the study area rasters, however, a buffer was created around the watershed's boundary so that the ridges are fully visible in Figure 2.2 and Figure 2.3, where the predictor variable rasters are depicted.

Planform curvature (also called plan curvature), calculated in SAGA GIS, describes the curvature perpendicular to the slope. In this study area, the values ranged from -.08 to .06 radians, where negative values are concave and positive values are convex. RSP values for the plots in this study area range from 0 to 1, with 0 indicating a low slope position and 1 indicating a ridge slope position. Slope, in degrees, ranged from 0 to 45-degree slopes. Solar radiation was calculated in ArcGIS from day 91 to 305 in the Julian calendar. Southwestness was used in place of aspect, which was calculated by cosine ((aspect – 225)/180 * pi), where aspect is measured in degrees. The values in this study area range from -1 to 1. A value of 1 indicates that the site is southwest-facing, while a value of -1 indicates that the site is northeast-facing. TWI was calculated using the d-infinity algorithm used (Tarboton 1997). For this study area, the TWI values range from 1 to 21, where 1 indicates the driest site and 21 would indicate a site with the most moisture.

The CWB metrics were calculated using a 1.5-meter LiDAR-derived DEM. Soil water-holding capacity for the study area was procured from the Natural Resource Conservation Service (NRCS) Soil Survey Geographic Database (SSURGO) (NRCS 2019). These soil properties are average estimates of the top 100 cm of soil, with a resolution of 1:12,000 to 1:63,360. Climate data for each month of summer of 2019, including precipitation totals, average temperature, total solar radiation, and average relative humidity, were downloaded from the Kentucky Mesonet Quicksand weather station, approximately 16 km away from the study area (Kentucky Mesonet 2019). The solar radiation was converted from MJ/m², the unit of the monthly Kentucky Mesonet solar radiation data, to Wh/ m², the unit required by the CWB toolset, using (MJ/ m² *

277.778). The relative humidity recorded by Kentucky Mesonet reflects maximum and minimum values for each month, the mean value was calculated to represent the monthly temperature. The soil moisture data (GWC and TDR) were collected throughout July 2019, therefore the CWB outputs from July 2019 were used for analysis.

Statistical Analysis

R version 3.5.1 (R Core Team 2018) and a significance level of 0.05 was used for all statistical analysis. To quantify the relative influence of three terrain factors, slope aspect, topographic position, and slope curvature, on soil moisture variability three-way ANOVAs were calculated for GWC and TDR. Type III ANOVA models were examined to determine factor significance using the *Anova* function in the car package (Fox and Weisburg 2011). The *lrtest* function from the lmtest package (Zeileis and Hothorn 2002) was used to calculate the log-likelihood ratio test of the full model with all interactions including the three-way interaction and the model with main effects and two-way interactions. Tukey pairwise comparisons of estimated marginal means were calculated using functions in the emmeans package (Lenth 2019). In addition to the soil moisture data, means and standard errors for the soil properties were calculated for each sampling strata (slope aspect, slope curvature, and topographic position).

To assess and compare the explanation power and model performance of commonly used GIS terrain and CWB variables in explaining soil moisture model averaging and stepwise AIC approaches were used. Linear models were created using the *lm* function in the stats R package (R Core Team 2018). There were three model categories in the analysis framework: terrain, CWB, and the combination of variables in terrain and CWB categories. The terrain model category includes RSP, SW, slope

steepness, TWI, plan curvature, and solar radiation (Figure 2.2). The CWB model category includes PET, storage, and surplus (Figure 2.3). There was not a deficit in July of 2019, therefore, deficit was not used in the modeling framework. The third model category is a combination of the variables from the previous two categories (terrain and CWB). Two metrics of soil moisture were used including GWC and TDR.

A model averaging approach was used to identify the importance of each variable in the three model categories for each soil moisture metric. The *dredge* function in the MuMIn package (Barton 2019) was used to rank the variables in each model category by their sum of weights. Delta AICc < 4 was used to define the subset of models, therefore, each variable's sum of weight was calculated for this subset of models.

To compare the performance of CWB variables to easily derived GIS variables, stepwise AIC identified the combination of variables from each model category that best explains the soil moisture metric. The *stepAIC* function in the MASS package (Venables and Ripley 2002) was used to identify these top models for each soil moisture metric within each model category. Fit statistics for these top models were then recorded, including f-statistics and multiple R^2. To formally compare the performance of each of these top models to one another, the *vuongtest* function in the nonnest2 package was used (Merkle and You 2018) to execute the non-nested likelihood ratio test for each of top models selected in the stepwise AIC approach. The *vuongtest* function tests the distinguishability of two models and subsequently indicates whether one model fits significantly better than the other.

RESULTS

The Pearson correlation coefficients of the in-field soil moisture measurements (Table 2.1) indicate that all methods of measurement were strongly correlated with correlation coefficients greater than 0.58. The 20 Micro Stations that recorded continuous measurements throughout the growing season were not used in statistical analysis as they represented a subsample of the 100 plots. Therefore, the data from the 100 plots was used in the model comparison. Both the GWC and TDR readings had high correlations and positive relationships with the Micro Station readings for the corresponding times (Figure 2.4).

Soil Moisture Analysis of Variance

The means and standard errors of TDR and GWC measurements by each factor level are found in Table 2.2. The volumetric water content readings from the TDR and the readings from GWC show a decreasing amount of soil moisture moving upslope, however, the driest slope position among the TDR readings is the upper slope, while the ridge is the driest slope position among the GWC readings. The soil moisture reading trends between slope aspects are not the same between TDR and GWC, as the TDR shows the southwest-facing slope being slightly wetter than the northeast-facing slope. This trend is reversed in the GWC measurements where the northeast-facing slope has a higher GWC mean value compared to the southwest-facing slope. For both soil moisture measurements, the concave sites have greater soil moisture than the convex sites.

The results of the three-way ANOVA for TDR indicated that there is not a significant three-way interaction. The log-likelihood ratio test was implemented to determine whether there was a significant difference between the full model with all

interactions (two-way and three-way) and the reduced model (the three-way interaction was dropped, but the main effects and two-way interactions were kept). The results of the log-likelihood ratio test indicated that there is a significant difference ($p = 0.02$) between the full model and reduced model. Therefore, the full model was used in the post-hoc analysis. There is a significant interaction between topographic position and curvature in the full model, but the other two-way interactions were not significant. The Tukey pairwise comparison of topographic position and curvature reveals significantly higher moisture content on valley concave slope positions compared to concave ridge positions (Table 2.3). The differences within convex transects are more nuanced than that of concave transects, with the valley position having significantly greater moisture compared to the other slope positions, but the upper slope position, instead of the ridge, is the driest. Additionally, the lower slope is significantly drier than the valley slope position. When comparing the soil moisture of different curvatures within topographic positions, only the upper slope position has a statistically significant difference between the concave and convex sites (Table 2.3). There was not a significant interaction between topographic position and aspect for the TDR measurements, however, to compare spatial trends for TDR to GWC, Table 2.4 illustrates mean and standard error for TDR measurements between aspect and topographic position. The TDR measurements reflect that moisture increases downslope on the northeast-facing slope. The southwest-facing slope follows a similar pattern, however, the driest topographic position on the southwest-facing slope is the upper slope and not the ridge. There are not large differences between the corresponding topographic positions on the opposing slope aspects.

The three-way ANOVA for GWC did not indicate a significant three-way interaction. The log-likelihood ratio test was implemented to determine whether there was a significant difference between the full model with all interactions, including the three-way interaction, and the reduced model (in which the three-way interaction was dropped, but the main effects and two-way interactions kept). A log-likelihood ratio test was performed for the full and reduced model (with main effects and two-way interactions) and found that there was not a significant difference ($p = 0.17$), therefore, the reduced model was used in subsequent analysis. The ANOVA of the reduced GWC model indicated that there are significant interactions between aspect and slope curvature ($p = 0.02$) and aspect and topographic position ($p = 0.02$), however, the interaction between topographic position and curvature is not significant. The Tukey pairwise comparisons for these significant interactions indicate that among concave sites, the northeast-facing aspect has significantly more moisture than the southwest-facing slope, but there are not significant differences between aspects in convex sites (Table 2.5). Within the northeast-facing slope, there is a significant difference between concave and convex sites. The Tukey pairwise comparison between aspect and topographic position indicates within the northeast-facing aspect the ridge topographic position is significantly drier than the other topographic positions (Table 2.6). Additionally, within the topographic positions, valley and lower slope sites have significantly greater moisture on the northeast-facing slope compared to the southwest-facing slope (Table 2.6).

Soil Properties

The descriptive statistics of soil properties by sampling strata can be found in Tables 2.7 through 2.9. The northeast slope has higher values of pH, total nitrogen, total

carbon, and greater concentrations of soil nutrients including Ca, Mg, Zn, P, and K (Table 2.7). The sand concentration is greater on the northeast-facing slope, while silt and clay are higher on the southwest-facing slope. The mean and standard error of soil properties by curvature are in Table 2.8. Soil moisture, represented by both GWC and TDR, is higher on concave sites. Concave sites have higher pH values, as well as higher total nitrogen, total carbon, and nutrient concentrations including Ca, Mg, Zn, P, and K. Concentrations of sand are greater on convex sites, while silt and clay concentration are greater on concave sites. Means and standard error of soil properties for the five topographic positions used in the sampling strata are in Table 2.9. Lower slope positions (valley, lower slope, and middle slope) have higher pH values compared to the upper slope and ridge positions. Ca and Mg concentrations are greatest in the lower slope positions (valley and lower slope) and decreased with increasing topographic positions. Sand concentrations were highest in the valley and decreased moving upslope. Silt and clay concentrations were generally highest in ridge positions and decreased moving downslope.

Model Averaging

The results of model averaging (Table 2.10) indicate the ranking of variables based on their sum of weights in models with delta AICc < 4. For each soil moisture metric, RSP has high importance. RSP was the top variable for each soil moisture metric in the GIS terrain category and within the top two variables in the combination category. For GWC, RSP was followed by southwestness in both the terrain and combination categories. In the CWB model category, our results suggest that storage is the top-performing CWB variable for each of the soil moisture metrics, followed by PET and

surplus. Both GWC and TDR have storage as a top-ranking variable in the combination category, it ranks third for GWC and first for TDR.

Model Comparison

The results of the stepwise AIC approach, which identifies the combination of variables that best explains each soil moisture, are found in Table 2.11. The top-performing models for each model category and the corresponding F-statistic and R^2 are also in Table 2.11. While the R^2 values indicate the strength of the relationship between the predictor variables and the response variable, the F-statistic indicates whether the linear regression model is better fit to the data compared to the null model. The F-statistic is influenced by the degrees of freedom, which should be noted as each of the models within and among the metrics have different numbers of predictor variables.

Among the top terrain models for each soil moisture metric, RSP is the top-ranking variable and has a negative relationship with soil moisture, indicating that as RSP increases, soil moisture decreases. For TDR, slope was the second variable in the terrain top model. The top CWB model for each soil moisture metric solely contains storage and the relationship between soil moisture and storage is positive. For the combination model, the ordering of variable significance is different for each soil moisture metric, however, there is overlap in variables. For GWC the variables include RSP, solar, PET, storage, and plan curvature, while for TDR the variables include slope, storage, RSP, solar, and PET.

In general, the terrain top models have greater R^2 values than the corresponding CWB top models for each of the soil moisture metrics. Additionally, the top combination models have greater R^2 values than both the corresponding terrain and CWB models. The

results of the formal comparison of the top models for each moisture metric, using the non-nested likelihood ratio test, are in Table 2.12. For both GWC and TDR measurements, the fit of the top terrain and CWB models are not statistically different, while the combination model fit significantly better than the corresponding CWB model. In general, the combination model fits better than the terrain model for all soil moisture metrics, as the R^2 values are greater for the combination models (Table 2.11), however, these differences are not significant per the non-nested likelihood ratio test (Table 2.12).

DISCUSSION

Our results suggest that models with solely CWB variables do not perform better than models with easily derived GIS terrain variables in explaining soil moisture, however, the differences between these models are not substantial. Additionally, the inclusion terrain variables with CWB variables in the combination model significantly improves model performance in explaining soil moisture variability when compared to CWB variables alone. Among the CWB variables used in the model averaging and stepwise AIC framework, storage is a top-performing variable in comparison with PET and surplus for explaining soil moisture. RSP is a top-performing variable among the terrain variables.

Patterns of Soil Properties

As many ecologists have studied, the topography of dissected landscapes can play an important role in hydrological and erosional processes, including mineral weathering, leaching, sedimentation, and soil erosion (Moore et al. 1993). Terrain features, specifically, slope aspect, slope curvature, and upslope area have been studied for their effects on soil moisture and flow patterns (Seibert et al. 2007). The patterns of soil moisture as documented by TDR and GWC measurements differ slightly from one another, which is reflected by the ANOVA and Tukey pairwise comparison results. The results for TDR suggest that slope curvature and topographic position significantly influence soil moisture patterns. Concave sites had a significant difference between ridge and valley positions, while the convex sites had more nuanced differences. The general pattern among topographic positions is similar for both convex and concave sites with significant differences between the valley and all other slope positions.

The GWC measurements highlight the effects of topographic position, slope aspect, and slope curvature on soil moisture. Two differences lie within the northeast-facing slope sites, where the ridge positions were significantly drier than valley positions and concave sites were significantly more moist than convex sites. Additionally, concave sites were significantly moister on the northeast-facing slope compared to the southwest-facing slope. Lastly, there was significantly greater moisture within the valley and lower slope positions on the northeast-facing slope compared to the southwest-facing slope.

There are slight variations between the two methods of soil moisture measurement. For example, the TDR measurements do not reflect a significant difference in moisture between slope aspects, whereas the GWC measurements reflect this difference. These differences are illustrated in Table 2.4 and Table 2.6. In general, both soil moisture metrics, TDR and GWC, reflect that moisture is greater on the northeast slope, except for the ridge positions where the northeast ridge is drier than the southwest ridge for both TDR and GWC. However, these moisture differences between slope aspects are not as pronounced in the TDR measurements, explaining why slope aspect was not included in significant interactions for TDR.

Despite this difference in spatial trends between TDR and GWC, the effects of terrain on soil moisture patterns are evident. Differences among topographic positions are apparent in both the TDR and GWC measurements, namely soil moisture is greater at lower slope positions compared to upper slope positions. As noted by others, lower slope soils experience less evaporative demand (Aandahl 1949; Bates 1923) and cooler temperatures (Franzmeier et al. 1969). Topography modifies the distribution of materials downslope, including leaching of nutrients and solid materials, leading to higher pH

(Giesler et al. 1998; Kalisz 1986), and more organic matter (Aandahl 1949), as well as thicker sola and soil horizons (Cooper 1960) at lower slope positions. Seibert et al. (2007) noted that the correlations between soil chemistry and topography were higher for the O horizon, citing the control of topography was greater since the organic layer is exposed. These results may also indicate that the soil chemistry is influenced by vegetation in addition to topography (Seibert et al. 2007). For example, Kalisz (1986) noted that exchangeable calcium concentrations were greater where *Liriodendron tulipifera* was found due in part to the higher level of Ca levels in the foliage. Through leaching and litterfall, the concentrations of Ca were higher in the surrounding surface soil, noting that the chemical properties of the A horizon are reflecting species composition rather than controlling it (Kalisz 1986). The combined effects of microclimate and movement of materials downslope favor the ability of lower slope positions to accumulate and retain soil moisture. Topographic position influences many ecological processes, which is reflected by both the patterns of soil moisture and soil properties in this Appalachian watershed.

Variable Performance and Comparison

Comparison of the top models from stepwise AIC suggests that the CWB models do not explain soil moisture variability better than easily derived GIS terrain variables, however, the non-nested likelihood ratio test indicates that these differences are not significant. The inclusion of terrain variables with CWB variables significantly improves model fit when compared to CWB variables alone. The model averaging results, which indicate the ranking of variables, emphasize the importance of solar radiation and topographic position in controlling patterns of soil moisture. As reflected by the ANOVA

and Tukey pairwise comparison results for TDR and GWC, the processes most important in explaining soil moisture patterns for these two different moisture metrics differ slightly. RSP is the top variable in the terrain category for TDR and GWC, and among the top variables in the combination category for both soil moisture metrics. Other variables that performed well in the model averaging and model selection framework include CWB storage, southwestness, slope steepness, and plan curvature.

Of the CWB variables, storage was the top variable for TDR and GWC. Dyer (2009) investigated the ability of CWB storage to explain soil moisture patterns in North Carolina and Ohio reported correlation coefficients between CWB storage and a relativized soil moisture metric from 0.92 to 0.97. The correlation coefficient between CWB storage and the soil moisture measured in this study are lower, with TDR having a Pearson correlation coefficient of 0.46 and GWC having a coefficient of 0.52. The sampling sizes, sampling patterns, and methods did differ between these two studies. Our study had 100 plots, while the North Carolina study area had nine plots and the Ohio site had 19 from Dyer (2009). Additionally, the depth at which measured soil moisture and soil properties were measured in this study differed from Dyer (2009). In the North Carolina sites, the soil moisture was measured at 30-60 cm and 50 cm at the Ohio sites (Dyer 2009), while the depth at which soil properties and soil moisture were measured was approximately 10 cm for this study. Previous studies have shown that the influences of topography on soil moisture decrease with soil depth (Florinsky et al. 2002; Lookingbill and Urban 2004; Yeakley et al. 1998), which could be a possible reason that topographic position did not seem to influence patterns of soil moisture in Dyer (2009).

Topographic position (represented by RSP in this study) is not currently integrated into the current CWB toolset's calculation of available water, which appears to explain some soil moisture variability in the forested watershed from this study. Without using topographic position in the calculation of CWB metrics, the influences of topographic position on drainage and other ecological processes influencing the accumulation and retention of moisture could be underrepresented by the CWB toolset. The spatial pattern of the CWB storage may roughly mimic the spatial pattern and effects of topographic position. The NRCS SSURGO database AWC data, used in calculating CWB storage, has a coarse resolution. For this watershed, there are three AWC values spatially divided by ridge, north-facing aspect, and south-facing aspect. Though user-provided soil data would likely provide higher resolution data, many users will not be able to feasibly provide soil data for their study area. Moore et al. (1993) noted that soil survey maps and databases generally have resolutions lower than that needed for detailed environmental modeling, which is reflected by our results. However, as Moore et al. (1993) concluded, the integration of terrain attributes with soil survey maps and databases, by using DEMs, may be more beneficial for landscape-scale modeling.

The importance of topographic position in explaining patterns of soil moisture may be seasonal and site-specific. The spatial organization of soil moisture and the processes controlling these factors are expected to change throughout the year. In Australia, Western et al. (1999) found during wet periods, the spatial pattern of soil moisture reflected topographic controls and a strong degree of spatial organization. When moisture availability is low, however, this spatial pattern is less evident and soil moisture patterns reflected differences in evapotranspiration, represented by a potential radiation

index in the Western et al. (1999) study. A combination of variables, including ln(a), where a is the upslope area, or ln(a/tan(β)), where β is the surface slope, and the potential solar radiation index explained 61% of the variation in soil moisture in the wet season and 22% during the dry periods. During dry periods, the potential radiation index showed the strongest relationship with soil moisture. For Australia, the winter months were characterized as being wet, while the summers were characterized as the dry periods with little spatial organization attributed to topography.

The control of surface topography on the spatial variability of flow dynamics in wet periods, compared to negligible effects during dry periods, has been reported by other studies (Chirico et al. 2003). During seasons where deficit does occur, a single peak in the hydrograph can denote that no subsurface lateral flow is occurring (Burt and Butcher 1985). These findings may vary, however, as Famiglietti et al. (1998) reported the influence of topography on soil moisture variability increased as the soil dries.

Given the inherent differences among study areas, the current and future regional climate should be considered when assessing the applicability of this model in representing soil moisture patterns. The seasonality of temperatures and precipitation will influence the patterns of soil moisture and the processes causing these patterns. In Kentucky, there is often adequate precipitation during much of the growing season, increasing the likelihood that soil moisture is at or above field capacity. This was the case for July 2019, in which our soil moisture data was collected, however, it is possible to have years with growing season deficit. In regions that experience, or will experience, less precipitation during the growing season, the effects of topographic position on drainage may not be as pronounced, given the soils could be below field capacity.

Limitations and Future Work

There are many opportunities to expand and improve upon this work. The first consideration is that the soil moisture measurements used in this study, GWC and TDR, reflect one-time measurements throughout July 2019 as data collection occurred over several trips. Future studies could test the accuracy of CWB metrics throughout the year using long term sampling. Though time series data was recorded over five months in this watershed, it was not used in statistical analysis as the 20 plots were unique combinations from the factorial design. Additionally, this study focused on how GIS-derived variables, including CWB and terrain variables, could be used to explain soil moisture, not plant available water. Soil moisture alone does not reflect what water is available to plants and the depth at which soil moisture was measured in this study does not capture all the moisture available at rooting depth. Lastly, climate, parent material, and landform will greatly influence many of the processes and patterns discussed, therefore, the applicability of terrain and CWB variables in explaining moisture patterns in other study areas will vary.

CONCLUSION

Our results reiterate that patterns of soil moisture in this Cumberland Plateau watershed are influenced by topographic position, as well as slope aspect and slope curvature. RSP, a variable representing topographic position, performed well among the GIS-derived terrain variables in explaining soil moisture distribution. Storage performed well among the CWB variables, though the coarse spatial distribution of storage should be noted. The performance of terrain and CWB models individually are not significantly different in explaining soil moisture, however, the inclusion of terrain variables with CWB variables does significantly improve model performance compared to CWB variables alone. The inclusion of a topographic position variable in future iterations of a GIS CWB toolset may improve its ability to explain soil moisture variability. In highly dissected landscapes where steep slopes influence drainage and reflect other ecological patterns important to water availability, topographic position should be included to properly represent patterns of soil moisture.

The CWB toolset variables do present a major advantage over traditional GIS-derived terrain variables. CWB variables reflect temporally dynamic patterns of evaporative demand and available water through the incorporation of coarse climate data and fine-scale terrain data. Under changing climate conditions, dynamic variables, such as CWB, will become increasingly important as the spatial and temporal patterns of precipitation and temperature change.

Table 2.1 Pearson correlation coefficient between measured soil moisture methods.

	GWC (n = 100)	*Combined TDR (n= 100)*
TDR (n = 92)	0.58***	
Micro Station (n = 20)	0.58**	
Combined TDR (n = 100)	0.59***	
Combined Micro Station (n= 20)		0.60**

Computed correlation used pearson-method with pairwise-deletion.

Note: GWC and TDR measurements were taken at the same time, except TDR readings of 8 plots due to equipment malfunction. The Combined TDR measurements (n = 100) include the 8 plots recorded at a later date and the Combined Micro Station readings reflect the same time stamps as the Combined TDR.

Table 2.2 Volumetric Water Content from TDR and Gravimetric Water Content (%; mean ± SE) by each factor including topographic position (TP), slope aspect, and curvature.

Factor	Levels	Volumetric Water Content	Gravimetric Water Content
TP	Valley	23.01 ± 0.83	31.65 ± 1.13
	Lower Slope	18.98 ± 0.90	30.95 ± 1.39
	Middle Slope	18.07 ± 0.76	29.32 ± 0.91
	Upper Slope	14.92 ± 1.28	27.50 ± 1.27
	Ridge	15.31 ± 1.49	24.07 ± 1.39
Aspect	Northeast-facing	17.95 ± 0.92	30.41 ± 1.03
	Southwest-facing	18.16 ± 0.64	26.99 ± 0.54
Curvature	Concave	19.49 ± 0.63	30.30 ± 0.80
	Convex	16.62 ± 0.89	27.10 ± 0.86

Table 2.3 Volumetric Water Content (%) from TDR, mean ± SE, across topographic positions (TP) and slope curvature.

TP	Concave	Convex
Valley	22.70 Aa ±1.17	23.31 Aa ± 1.24
Lower Slope	20.34 ABa ± 1.14	17.61 Ba ± 1.29
Middle Slope	19.87 ABa ± 0.68	16.26 BCa ± 1.10
Upper Slope	18.21 ABa ± 1.62	11.63 Cb ± 1.35
Ridge	16.30 Ba ± 1.55	14.33 BCa ± 2.59

Note: Upper-case letters indicate significant differences between topographic positions within curvature classes. Lower-case letters indicate significant differences between curvature within topographic positions. Differences were determined by Type III ANOVA and post-hoc Tukey Pairwise comparisons.

Table 2.4 Volumetric Water Content (%) from TDR, mean ± SE, across topographic positions (TP) and slope aspects.

TP	Northeast-facing	Southwest-facing
Valley	23.85 ± 0.92	22.16 ± 1.39
Lower Slope	19.68 ± 1.48	18.27 ± 1.04
Middle Slope	18.18 ± 1.34	17.95 ± 0.78
Upper Slope	15.38 ± 2.22	14.45 ± 1.38
Ridge	12.68 ± 2.35	17.95 ± 1.50

Table 2.5 Gravimetric Water Content (%; mean ± SE) across slope aspects and slope curvature.

Aspect	Concave	Convex
Northeast-facing	33.12 Aa ± 1.22	27.71 Ab ± 1.51
Southwest-facing	27.48 Ba ± 0.67	26.49 Aa ± 0.85

Note: Upper-case letters indicate significant differences between aspects within curvature classes. Lower-case letters indicate significant differences between curvature within aspects. Differences were determined by Type III ANOVA and post-hoc Tukey Pairwise comparisons.

Table 2.6 Gravimetric Water Content (%; mean ± SE) across topographic positions (TP) and slope aspects.

TP	Northeast-facing	Southwest-facing
Valley	35.07 Aa ± 1.34	28.22 Ab ± 1.00
Lower Slope	34.15 Aa ± 2.17	27.75 Ab ± 1.10
Middle Slope	30.23 Aa ± 1.55	28.40 Aa ± 0.97
Upper Slope	29.57 Aa ± 1.92	25.43 Aa ± 1.49
Ridge	23.02 Ba ± 2.54	25.11 Aa ± 1.23

Note: Upper-case letters indicate significant differences between topographic positions within aspects. Lower-case letters indicate significant differences between aspects within topographic positions. Differences were determined by Type III ANOVA and post-hoc Tukey Pairwise comparisons.

Table 2.7 Soil properties by slope aspect (mean ± SE).

Soil Property	Northeast-facing	Southwest-facing
pH (Soil Water)	5.07 ± 0.07	4.62 ± 0.02
Total N (%)	0.18 ± 0.01	0.09 ± 0.003
Sand (%)	50.02 ± 2.17	44.4 ± 2.40
Silt (%)	36.39 ± 1.74	41.34 ± 1.96
Clay (%)	13.59 ± 0.52	14.25 ± 0.55
Total C (%)	2.26 ± 0.08	1.86 ± 0.06
Field Capacity (%)	33.51 ± 0.93	32.38 ± 0.73
Wilting Point (%)	15.29 ± 0.60	13.15 ± 0.51
Plant Available Water (%)	18.23 ± 0.47	19.23 ± 0.52
Ca (mg/kg)	440.87 ± 48.13	107.43 ± 14.83
Mg (mg/kg)	101.46 ± 8.69	45.29 ± 4.80
Zn (mg/kg)	2.258 ± 0.16	1.33 ± 0.07
P (mg/kg)	5.91 ± 0.38	3.17 ± 0.15
K (mg/kg)	95.59 ± 5.20	64.6 ± 2.41

Table 2.8 Soil properties by slope curvature (mean ± SE).

Soil Property	Concave	Convex
pH (Soil Water)	4.88 ± 0.07	4.81 ± 0.05
Total N (%)	0.15 ± 0.01	0.12 ± 0.01
Sand (%)	41.81 ± 1.99	52.61 ± 2.40
Silt (%)	43.61 ± 1.66	34.13 ± 1.86
Clay (%)	14.58 ± 0.48	13.26 ± 0.60
Total C (%)	2.16 ± 0.08	1.96 ± 0.07
Field Capacity (%)	35.11 ± 0.75	30.78 ± 0.81
Wilting Point (%)	15.5 ± 0.55	12.94 ± 0.55
Plant Available Water (%)	19.61 ± 0.48	17.85 ± 0.49
Ca (mg/kg)	297.41 ± 46.26	250.89 ± 38.84
Mg (mg/kg)	85.21 ± 9.46	61.54 ± 5.95
Zn (mg/kg)	1.87 ± 0.13	1.71 ± 0.14
P (mg/kg)	4.65 ± 0.39	4.43 ± 0.31
K (mg/kg)	83.6 ± 5.03	76.59 ± 4.10

Table 2.9 Soil properties by topographic position (mean ± SE).

Soil Property	Valley	Lower	Middle	Upper	Ridge
pH (Soil Water)	4.94 ± 0.08	4.97 ± 0.10	4.92 ± 0.10	4.83 ± 0.11	4.55 ± 0.03
Total N (%)	0.14 ± 0.01	0.15 ± 0.02	0.14 ± 0.02	0.14 ± 0.02	0.11 ± 0.01
Sand (%)	55.03 ± 1.89	50.41 ± 2.67	46.03 ± 2.38	45.60 ± 4.01	38.98 ± 5.45
Silt (%)	31.77 ± 1.50	36.25 ± 2.23	40.65 ± 2.11	41.00 ± 3.35	44.67 ± 4.23
Clay (%)	13.2 ± 0.56	13.34 ± 0.60	13.32 ± 0.49	13.39 ± 0.77	16.35 ± 1.35
Total C (%)	1.75 ± 0.08	2.13 ± 0.12	2.00 ± 0.10	2.25 ± 0.16	2.15 ± 0.09
Field Capacity (%)	30.03 ± 1.06	32.12 ± 1.05	33.87 ± 0.88	33.93 ± 1.39	34.76 ± 1.85
Wilting Point (%)	13.57 ± 0.57	14.23 ± 0.77	14.01 ± 0.74	13.91 ± 0.94	15.37 ± 1.37
Plant Available Water (%)	16.47 ± 0.70	17.89 ± 0.67	19.86 ± 0.62	20.02 ± 0.87	19.39 ± 0.81
Ca (mg/kg)	350.45 ± 60.35	377.5 ± 80.06	302.3 ± 73.34	257.60 ± 72.66	82.9 ± 10.14
Mg (mg/kg)	94.95 ± 10.13	88.98 ± 13.52	84.40 ± 14.39	62.85 ± 14.58	35.7 ± 3.61
Zn (mg/kg)	1.76 ± 0.16	2.06 ± 0.30	1.76 ± 0.20	1.84 ± 0.27	1.56 ± 0.09
P (mg/kg)	4.68 ± 0.26	5.40 ± 0.62	4.48 ± 0.55	4.13 ± 0.63	4.03 ± 0.62
K (mg/kg)	84.00 ± 5.49	91.38 ± 9.34	82.58 ± 5.84	79.4 ± 9.27	63.13 ± 3.80

Table 2.10 Ranking of predictor variables by sum of weights for each soil moisture metric.

Metric	Model	Ranking*	Sum of Weights					
GWC	Terrain	RSP SW PC Slope Solar TWI	1.00	0.94	0.58	0.30	0.25	0.22
	CWB	Storage PET Surplus	1.00	0.45	0.23			
	Combination	RSP SW Storage PC PET Solar	1.00	0.79	0.75	0.56	0.36	0.32
TDR	Terrain	RSP Slope PC TWI Solar SW	1.00	0.56	0.39	0.19	0.17	0.16
	CWB	Storage PET Surplus	1.00	0.39	0.20			
	Combination	Storage RSP Slope Solar PET PC	0.95	0.86	0.78	0.58	0.51	0.35

*Only the top six variables in the Combination model are shown. The variables are listed in order of importance, also indicated by the Sum of Weights. Abbreviated variable names are as follows: relative slope position (RSP), southwestness (SW), plan curvature (PC), slope steepness (Slope), solar radiation (Solar), topographic wetness index (TWI), CWB storage (Storage), potential evapotranspiration (PET), CWB surplus (Surplus).

Table 2.11 Top models selected using stepwise AIC, within three GIS variable categories: Terrain, Climate Water Balance (CWB), and Combination, for each soil moisture metric.

Metric	Model	Top Stepwise Model*	F Statistic	R^2
GWC	Terrain	RSP + SW + PC	17.48	0.35
	CWB	Storage	35.97	0.27
	Combination	RSP + Solar + PET + Storage + PC	11.19	0.37
TDR	Terrain	RSP + Slope	15.15	0.24
	CWB	Storage	26.39	0.21
	Combination	Slope + Storage + RSP + Solar + PET	8.65	0.32

* Variables are listed in order of increasing p-value. Underlined variables have a negative relationship with the soil moisture metric. Abbreviated variable names are as follows: relative slope position (RSP), southwestness (SW), plan curvature (PC), slope steepness (Slope), solar radiation (Solar), topographic wetness index (TWI), CWB storage (Storage), potential evapotranspiration (PET), CWB surplus (Surplus).

Table 2.12 Non-nested likelihood ratio test results for top models selected by stepwise AIC in the three GIS variable categories: Terrain, Climate Water Balance (CWB), and Combination.

Metric	Non-nested Likelihood Ratio Test	
GWC	Terrain fits better than CWB	p = 0.098
	Combination fits better than CWB	**p = 0.014**
	Combination fits better than Terrain	p = 0.241
TDR	Terrain fits better than CWB	p = 0.344
	Combination fits better than CWB	**p = 0.028**
	Combination fits better than Terrain	p = 0.057

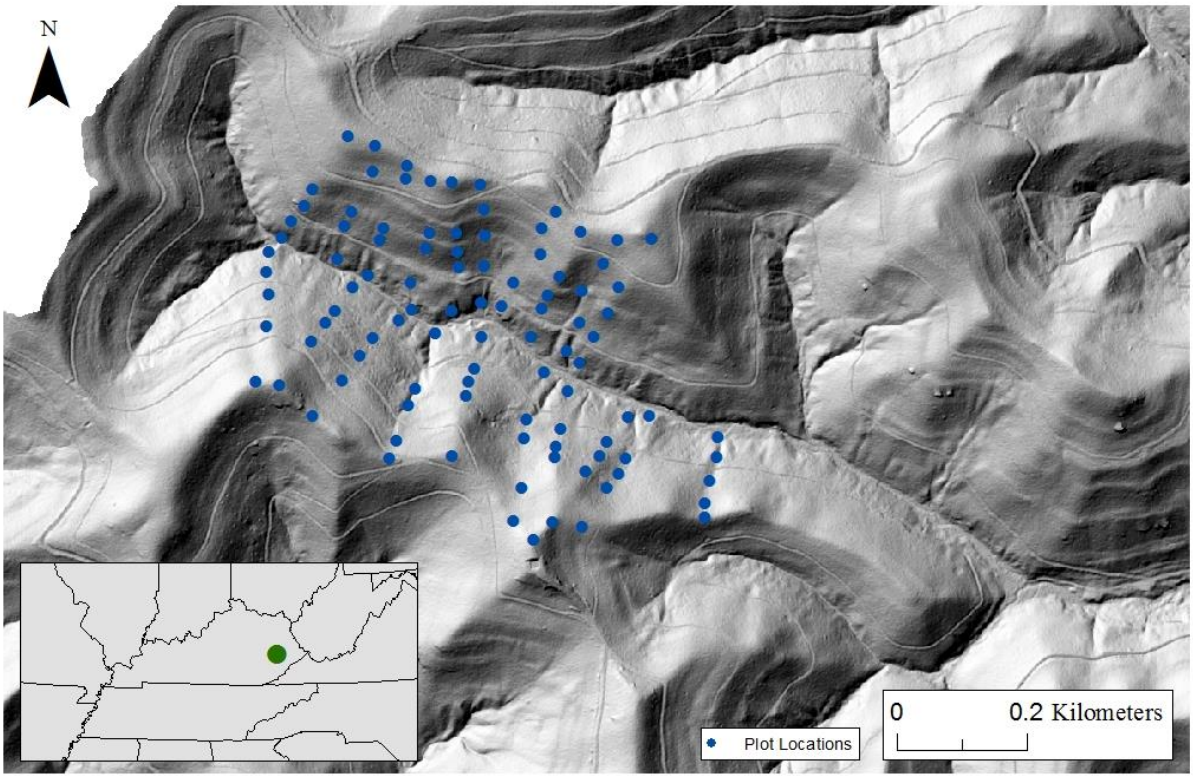

Figure 2.1 Plot locations in Little Millseat watershed located in Kentucky, USA.

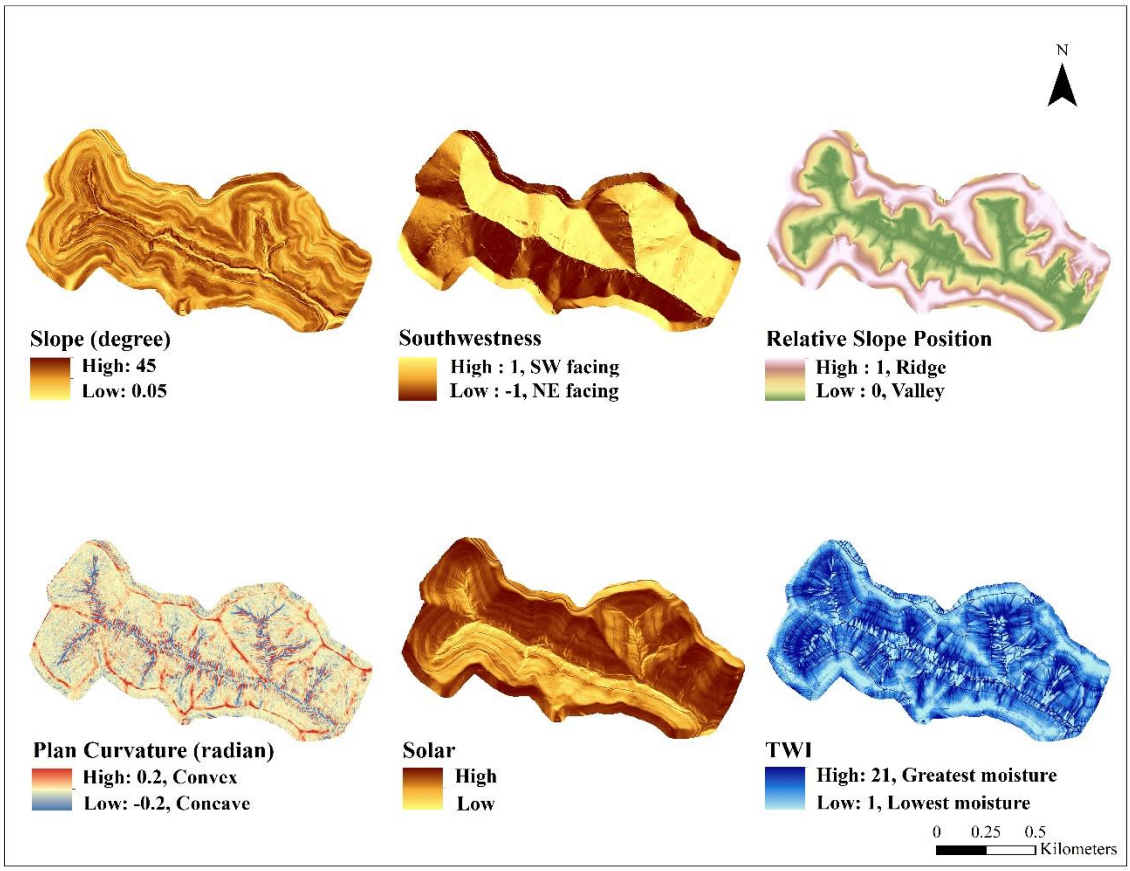

Figure 2.2 GIS terrain variables used in the terrain category, from left to right, top to bottom: Slope, Southwestness, Relative Slope Position, Plan Curvature, Solar, and Topographic Wetness Index (TWI).

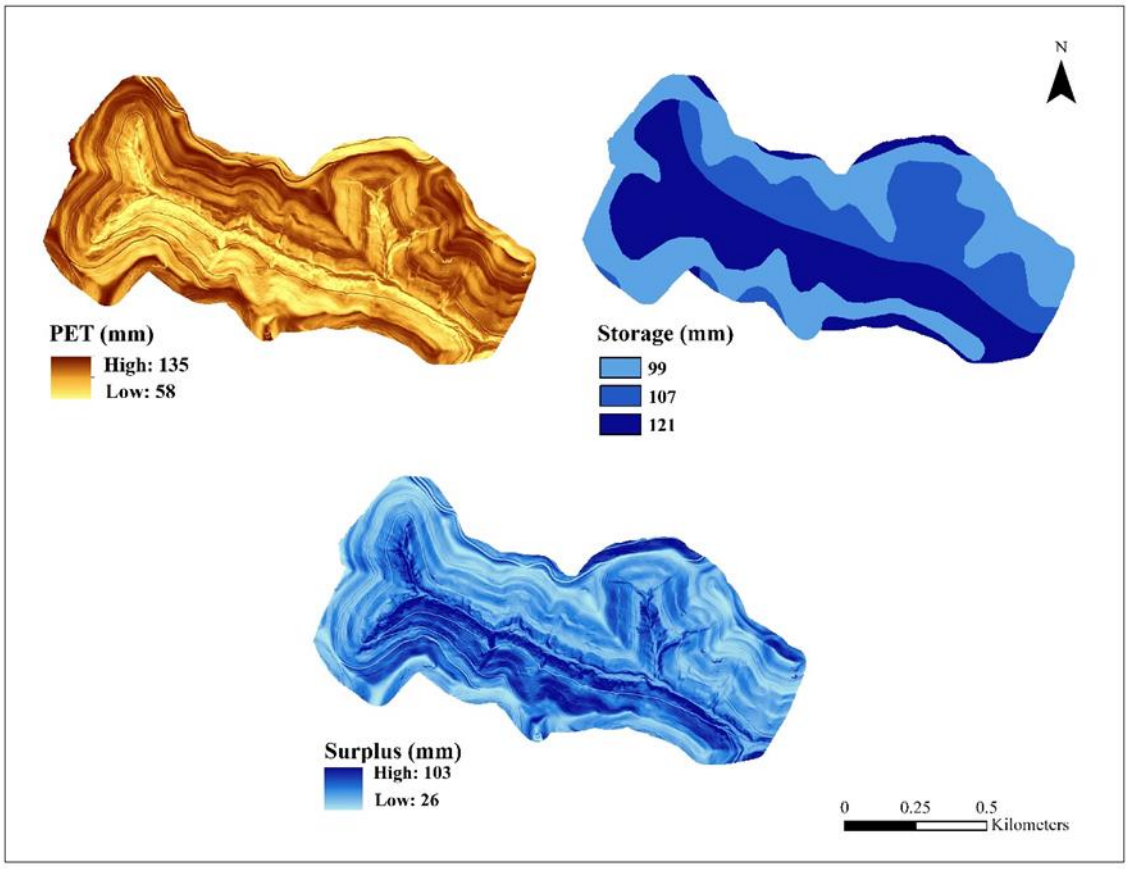

Figure 2.3 GIS Climate Water Balance (CWB) variables used in the CWB category, from left to right, top to bottom: PET, Storage, and Surplus. CWB variables reflect calculations for July 2019.

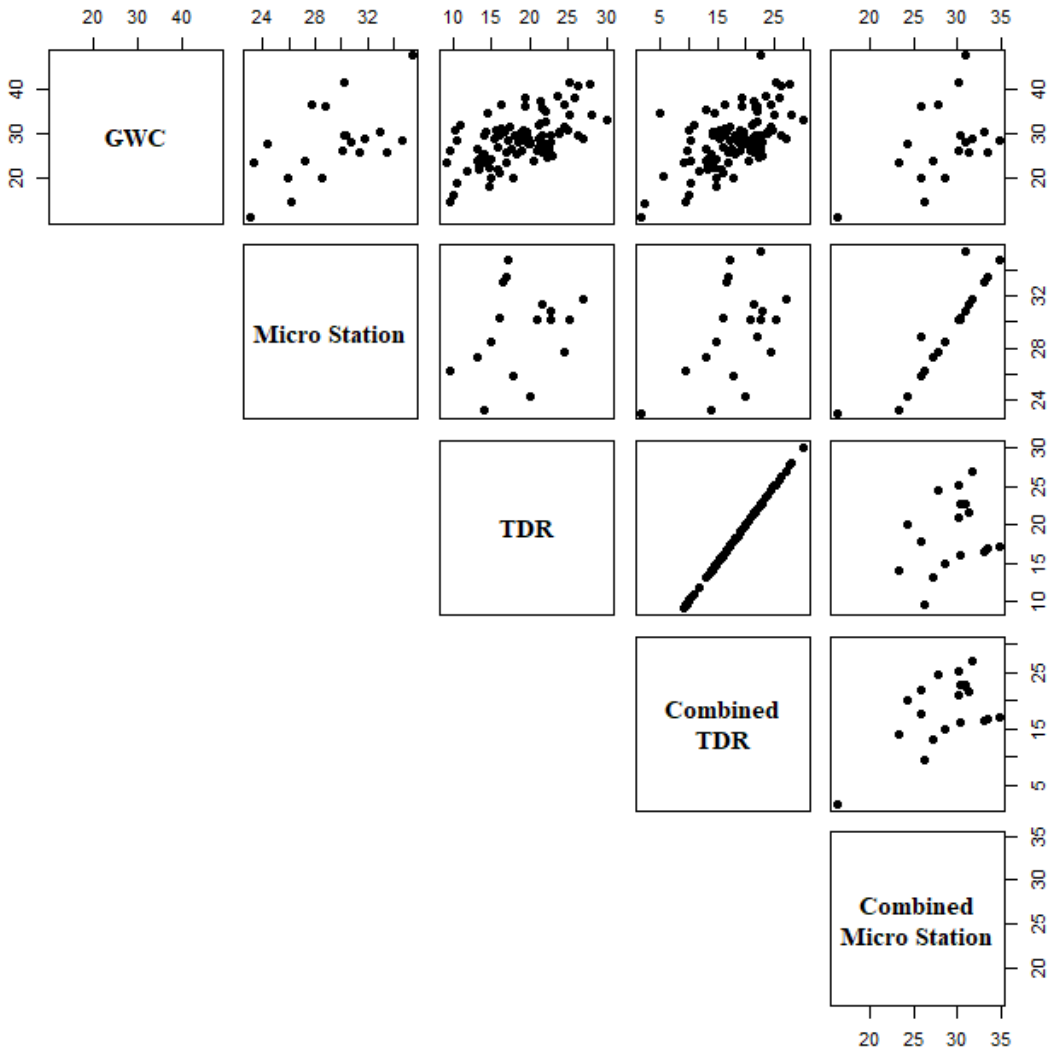

Figure 2.4 A scatterplot matrix of the soil moisture measurements collected for this study. Note: GWC and TDR measurements were taken at the same time, except TDR readings of 8 plots due to equipment malfunction. The Combined TDR measurements (n = 100) include the 8 plots recorded at a later date and the Combined Micro Station readings reflect the same time stamps as the Combined TDR.

CHAPTER 3 SPECIES DISTRIBUTION PATTERNS

INTRODUCTION

Climate Change and Shifting Vegetation Distributions

Changes in climate influence the phenology (Bertin 2008; Cleland et al. 2007; Doi and Katano 2008), productivity (Boisvenue and Running 2006), mortality (Allen et al. 2010; McDowell and Allen 2015), and spatial distribution of plants (Davis and Shaw 2001; Kelly and Goulden 2008). These are consequences of alterations in global atmospheric carbon dioxide concentrations, temperature, energy budget, atmospheric circulation, and water cycle (Collins et al. 2013). With different magnitudes of these alterations around the world, the ability of plants to adapt will vary. Additionally, climate change will influence the frequency, severity, and patterns of forest disturbances, including fires and invasion of native and nonnative pests, presenting more mechanisms of change in forest ecosystems (Seidl et al. 2017). Reduction in resistance and resilience of plants from these collective changes, at the individual, population, and community levels, can impact the surrounding ecology of the area through reduced diversity, alterations of community structure, and extinction (Jump and Penuelas 2005).

Shifts in species and population distribution in response to changing climate have been documented in recent decades from the regional scale to the landscape scale. Climate change presents a scenario where populations will need to adapt or track ideal climate envelopes under changing conditions, at a faster rate. Population movement occurs when populations are establishing beyond their current range, such as seed dispersal or assisted migration (Corlett and Westcott 2013). In the Eastern United States, climate change is projected to result in range contraction if current sites become

unsuitable and recruitment at the leading edge is slower than the collapse of the population in the range core (Zhu et al. 2012). The abundance of species near the boundary of the range is important in determining the success of migration, which places rare species at a disadvantage (Iverson et al. 2004b). Within landscapes, tree species may shift to different topographic positions to track suitable microclimate conditions (Crimmins et al. 2011; Hannah et al. 2014; Keppel et al. 2012). It was predicted that plant species would move uphill to track the changes in optimal thermal conditions in the context of climate change (Chen et al. 2011; Gottfried et al. 2012). In locations where water availability increases and exceeds the evaporative demand rate, species could be expected to shift their distributions downhill (Crimmins et al. 2011). Observed shifts within the landscape in the Crimmins et al. study (2011) were a result of trees following water availability downslope, rather than solely tracking changes in temperature. Additionally, several studies in California have recorded the density of younger trees at lower elevations increasing in the last century (Crimmins et al. 2011; Eckert and Eckert 2007; Millar et al. 2004). Changes in climate and the subsequent effects on plants requires an investigation of what factors drive species distributions (Lenoir and Svenning 2015).

Gradient Analysis and Tree Species Distribution

Interpreting and predicting current and future species distributions in complex landscapes can be difficult. General plant community patterns have been recognized within regions or landscapes (Braun 1942; Whittaker 1956), however, the compound influences of terrain and microclimate on species distributions are not as easily parsed. Mountainous landscapes experience changes in gradients over small areas because of

high relief topography. North and south-facing slopes may have similar elevation, latitude, and macroclimate conditions, but the effects of topography on solar radiation, soil moisture, soil properties, and temperature can result in different plant communities on each slope (Bailey 2009). For example, in the Appalachian region, Oak-Hickory communities can be found on south-facing, drier slopes, and Beech-Maple communities on north-facing, mesic slopes (Hutchins et al. 1976).

Many studies have highlighted the importance of soil nutrients and topographic variables in influencing vegetation distributions (Franklin et al. 1993; Whittaker 1967). In western Kentucky and Tennessee, key environmental variables explaining tree species distributions along a forest continuum model include available water capacity, slope position, soil pH, elevation, and percent rock (Fralish et al. 1993; Franklin et al. 2002). Soil pH increases from xeric to mesic sites and nutrient availability is often greater on mesic sites compared to xeric sites (Muller and McComb 1986). Higher nutrient availability on mesic sites is attributed to higher rates of litter turnover compared to that of xeric species like *Quercus* spp. (Muller and McComb 1986; Peterson and Rolfe 1982).

In order to better understand the effects of changing climate on these ecosystems, environmental gradients that capture the dynamic conditions of changing climate and the intricate terrain of mountainous areas are needed. Gradient analysis has been a long-standing approach to understanding the ecology of a place. The distribution of resources throughout space influences the distribution of organisms, populations, communities, and ecosystems (Whittaker 1967). The role of topography in controlling species distribution, microclimates, and plant resources has been a focus of ecology since early gradient analysis. Vegetation surveys along transects can reveal how major plant communities

change with gradients such as elevation, slope, aspect, and topographic position (Whittaker 1967). Elevation and aspect, two commonly used and easily derived gradients, have been used to study vegetation distribution, however, the disadvantage of these variables is that they are not directly associated with the physiological responses or needs of plants. Under projected climate changes, these variables would not change. Physiologically pertinent variables, such as solar radiation, water availability, and temperature, covary with topographic gradients like aspect and elevation, but could be better suited when studying species distributions under changing climate (Lookingbill and Urban 2004; Stephenson 1990).

Climate Water Balance Concept

The concept of plant relevant gradients has been incorporated into spatially explicit metrics, using Geographic Information Systems (GIS), to capture ecologically pertinent patterns such as moisture distribution and drainage in landscapes. Two of the common GIS-derived moisture metrics are the topographic wetness index (TWI) (Beven and Kirkby 1979) and integrated moisture index (IMI) (Iverson et al. 1997). TWI is a relative moisture gradient that is calculated using the upslope contributing area and slope steepness of the site. IMI uses solar radiation potential, flow accumulation of water downslope, the curvature of the landscape, and the soil's total available water capacity. Though patterns of soil moisture have been shown to correlate with TWI (Beven and Kirkby 1979) and IMI (Iverson et al. 2004a), they do not physically quantify moisture amount (Dyer 2009). Additionally, TWI and IMI could not be used as a comparative metric for sites in different landscapes and remain static variables across time. These metrics have been helpful in capturing the pattern of water movement and moisture

gradients throughout a landscape, but the use of temporally dynamic variables is needed to fully capture the water availability at a site.

To address the need for plant relevant and temporally dynamic variables, many ecologists used climate metrics such as annual energy supply and annual water supply or the ratio of the two (Budyko et al. 1974; Holdridge 1967; Lieth 1975; Mather and Yoshioka 1968; Stephenson 1990; Whittaker and Likens 1975). These annual metrics are not as informative as the simultaneous availability of energy and water in a given time of the year. Additionally, locations can have similar annual energy and water supply, but different timing of these resources. As Stephenson (1990) noted, without energy the available water is not utilized; likewise, without water energy cannot be used for growth.

The climate water balance (CWB) concept accounts for the simultaneous availability of energy and water to plants (Stephenson 1990). Available water is water that the plants can utilize, which incorporates the water holding capacity of the soil. Not all water that enters the system through precipitation is held, as the ability of different soil types to hold water varies. Potential evapotranspiration (PET) is the rate at which evapotranspiration would occur when water is not a limiting factor. Many calculations of evapotranspiration use a standard crop to calculate this rate, though this rate is not static across plant types (Monteith 1965; Stephenson 1990; Thom 1975). PET is influenced by the amount of energy available and is quantified by using temperature, solar radiation, humidity, and wind speed data (Jensen and Allen 2016). Considering the available water and the amount of energy informs actual evapotranspiration (AET). When the water available to the plant does not meet the evaporative demand, AET is less than PET, there is a climate water deficit. Conversely, when the available water is more than what is

needed to fulfill the evaporative demand of PET, there is a water surplus (Stephenson 1990).

CWB metrics have been shown to represent several ecological patterns. AET is correlated with tree species richness (Currie 1991; Currie and Paquin 1987), net primary production (Lieth 1975; Rosenzweig 1968), and litter decomposition rates (Berg et al. 1993; Dyer et al. 1990; Meentemeyer 1978). Vegetation biomes can be differentiated by mean AET and mean deficit at the global scale (Frank and Inouye 1994) and in North America (Stephenson 1990). Likewise, AET in conjunction with deficit differs between tree species (Lutz et al. 2010).

GIS Climate Water Balance

With technological advances, CWB metrics can be calculated for large areas with fine spatial resolution. Extensive climate, soil, and terrain data have become pervasive and open to the public, creating opportunities to use technology and readily available data to calculate these topographic and climate properties that scientists in the 20th century were unable to use with such ease. Light Detection and Ranging (LiDAR)-derived digital elevation models (DEMs) with fine resolution allows scientists to access detailed spatial information for large spatial scales. Many terrain indices can be derived from a DEM using GIS software such as ArcGIS and SAGA GIS including moisture indices (topographic wetness index, climate water balance, relative slope position, topographic position index), solar radiation indices (aspect, solar radiation, southwestness), and terrain (slope curvature, slope steepness).

Dyer (2009) developed an ArcGIS toolset that implements the CWB concept with the ability to consider a given area's topography. This GIS toolset allows for the

calculation of the CWB from input data including a DEM of the study area, soil available water capacity (AWC), monthly temperature, monthly precipitation, and solar radiation (Dyer 2009). The toolset allows for data inputs to be user-provided or downloaded through agencies such as the National Resources Conservation Service (NRCS 2019) and PRISM Climate data (PRISM Climate Group 2019). This toolset uses the Thornthwaite approach (Mather 1978) for calculating components of the hydrologic cycle. For calculation of PET, this toolset uses the Turc equation (Turc 1961) which considers air temperature and solar radiation. A radiation-based method was chosen as this toolset aimed to investigate how topography influences moisture demand (Dyer 2019).

The CWB toolset produces many rasters including monthly and annual PET, AET, storage, deficit, and surplus. These rasters highlight how slope and aspect influence spatial patterns of solar radiation and PET. In validating the application of this CWB toolset for tree species distribution, Dyer (2019) found deficit values higher on ridges and side slopes in central Indiana, while mesic aspects had smaller deficits. In the ≥ 30 cm size class of trees, *Quercus alba*, *Quercus montana*, *Quercus velutina*, and *Carya glabra* occurred on sites with higher deficit values, while *Acer rubrum*, *Acer saccharum*, *Fagus grandifolia*, *Liriodendron tulipifera*, *Nyssa sylvatica*, and *Quercus rubra* were found on sites with lower deficits (Dyer 2019).

The current GIS CWB toolset does not, however, consider the influences of topographic position on water movement and drainage when calculating water available to the site. The effects of topography on drainage were thought to be minimal during the growing season (Dyer 2009, 2019). In highly dissected landscapes the dismissal of drainage effects on available water may influence how CWB is estimated. Mountainous

and variable landscapes experience movement of water and development of soil properties that may influence the water available to a site. A thorough examination of the current CWB toolset's ability to explain tree species distributions within dissected, heterogeneous landscapes is lacking. Therefore, the overarching objective was to assess the current GIS CWB model's ability to explain tree species distributions in a heterogeneous landscape of central Appalachia. In order to address this objective, there are three specific objectives: 1. to assess and compare the explanatory power of commonly used terrain and CWB variables derived using GIS in modeling tree species distributions, 2. to evaluate the modeling performance of the models using GIS terrain variables alone, GIS CWB metrics alone, and the combination of terrain and CWB variables in predicting species presence, and 3. to compare the spatial patterns of species predicted by each of the models.

METHODS

Study Area

A forested watershed, Little Millseat, located in the Cumberland Plateau and the Appalachian Coalfields of southeastern Kentucky, USA is a dissected landscape conducive to studying the high variability of environmental gradients and the subsequent tree species distributions (Kalisz 1986). Little Millseat watershed is a subwatershed of Clemons Fork watershed found in the University of Kentucky's Robinson Forest, a deciduous broadleaf forest spanning 6,000 hectares. Prior to the procurement of the land by the University of Kentucky, extensive cutting of the forest occurred between 1908 and 1923 (Overstreet 1984). Additionally, some slopes were cleared of trees and used for agriculture in the 1800s, a practice that influenced the soils and subsequent tree species after these "old fields" succeeded back to forest (Kalisz 1986). Little Millseat watershed does not appear to have evidence of any old fields.

The landscape is characterized by steep slopes and soils developed through residuum or colluvium (Hutchins et al. 1976; Williamson et al. 2015). The underlying parent material is from the Breathitt Formation of Pennsylvanian age and consists of sandstone, shale, and siltstone (Hutchins et al. 1976; Hinrichs 1978; McDowell 1985). The 0 to 45-degrees slopes of Little Millseat watershed are predominantly northeast and southwest-facing aspects. The complex interaction between climate and topography impacts on microclimates, soil properties, and vegetation is evident in this study area (Abnee et al. 2004; Cremeans 1992; Hutchins et al. 1976; Kalisz 1986).

Experiment Design

Plot locations were determined using a three-way factorial design, with factors including aspect, topographic position, and slope curvature (Figure 3.1). Two aspects (northeast and southwest), five topographic positions (ridge, upper slope, middle slope, lower slope, and valley), and two slope curvatures (convex and concave) were considered. These strata were chosen due to their role in influencing soil moisture and soil attributes. With this sampling design, there are 20 unique combinations, which were replicated five times, resulting in 100 study plots.

ESRI ArcGIS for Desktop 10.6 (ESRI 2011) was used to derive the locations of the plots before going into the field. The middle section of Little Millseat watershed has predominantly northeast and southwest-facing slopes. Slope curvature was determined by viewing Topographic Wetness Index and hillshade maps which were derived from a 1.5-meter LiDAR-derived DEM. The topographic position classes were determined using the Topography Toolbox for ArcGIS (Dilts 2015). A circular neighborhood with a 100-cell search radius was used in this tool for computing the TPI. The TPI raster was then used to create five topographic positions (ridge, upper slope, middle slope, lower slope, and valley). The 100-cell radius search radius was selected after other search radii of equal or less value produced less spatially contiguous class distinctions.

Transects were created in ArcMap along the concave and convex features, with five convex/ five concave transects on the northeast-facing slope and five convex/five concave transects on the southwest-facing slope. The TPI output was then imported into ArcMap with the overlaid transects. Five plots were then placed along each transect, one per topographic position. For the ridge class, plots were placed at the uppermost part of the ridge, while the remaining classes were placed systematically in the center of the TPI

range for that class. Plots were moved in ArcMap if they were within 11 meters of any forest access road, to avoid the effects the roads may have on hydrology or disturbance history. Plots that were moved were done so in ArcGIS to retain a buffer greater than 11 meters from the road. Coordinates derived from these maps were then exported to Avenza Maps and used to navigate during fieldwork (Avenza Systems, Inc. Toronto, ON, Canada).

The plots were established in early May 2019, the plot centers were marked using fiberglass stakes, flagging, and metal numbered tags. For plots on ridge top positions, disturbance effects from mining or forestry operations in the adjacent watersheds (increased stem density and invasive species) prompted the relocation of some plots approximately nine meters downslope (while remaining in the ridge TPI class). The coordinates of the established plot centers were recorded using a SXBlue II GNSS GPS receiver (Geneq, Inc., Montreal, QC, Canada). XY accuracy for 99% of the plots was under two meters, one plot had a three-meter accuracy. The coordinates were imported into ArcGIS in the WGS 1984 (G1150) coordinate system and projected to NAD 1983 StatePlane Kentucky FIPS 1600 Feet.

Vegetation Sampling

A fixed area plot design was used with 1/50-hectare area, an approximate radius of 8 meters, though a Nikon Forestry Pro rangefinder was used for slope correction. Trees within the 100 plots with diameters at breast height (DBH) at or greater than 12.7 centimeters were identified to species and their DBH and canopy class determined.

Predictor Variables

Two GIS software programs, ArcGIS for Desktop 10.6 (ESRI 2011) and SAGA GIS (Conrad et al. 2015), were used to calculate the predictor variable rasters, all of which were derived from a 1.5-meter LiDAR-derived DEM. Slope steepness and solar radiation were calculated with ArcGIS for Desktop, topographic wetness index (TWI), relative slope position (RSP), aspect (used to calculate southwestness), and plan curvature were calculated with SAGA GIS. CWB metrics were calculated using the Water Balance Toolset version 3.0.2 (Dyer 2009) in ArcGIS for Desktop 10.6. Focal means were calculated for each of the rasters, using a 9 by 9 cell focal mean, as the radius of the plot was approximately 8 meters and the rasters' cell dimensions are 1.5 x 1.5 meters. The boundary of Little Millseat was delineated in ArcGIS and used in clipping the study area rasters. A buffer was created around the watershed's boundary to accommodate the focal mean area of ridge positions and to make the ridge positions more evident, as shown in the predictor variable rasters in Figure 3.2 and Figure 3.3.

Planform curvature (PC) describes the curvature perpendicular to the slope. In this study area, the plan curvature values range from -.08 to .06 radians, where negative values are concave and positive values are convex. The RSP values for this study area range from 0 to 1, with 0 indicating the lowest slope position and 1 indicating a ridge slope position. Slope steepness in this study area ranged from 0 to 45-degree slopes. Solar radiation in this study represents solar radiation from day 91 to 305 in the Julian calendar, which is April 1 to November 1, where greater values indicate more solar radiation. Southwestness (SW), which was used in place of aspect, calculated by cosine ((aspect – 225)/180 * pi), where aspect is in degrees. Southwestness values for this study area range from -1 to 1. A SW value of 1 indicates that the site is southwest-facing, while a value of

-1 indicates that the site is northeast-facing. TWI was calculated using the d-infinity algorithm (Tarboton 1997). For this study area, the TWI values range from 1 to 21, where 1 indicates the driest site and 21 would indicate a site with the most moisture.

For calculating CWB metrics, the only user input provided in this study was a 1.5-meter LiDAR-derived DEM. Other data used in the model were from online sources or calculated by the model. Soil water-holding capacity was procured from the Natural Resource Conservation Service (NRCS) Soil Survey Geographic Database (SSURGO) (NRCS 2019). These soil properties are average estimates of the top 100 cm of soil, with a resolution of 1:12,000 to 1:63,360. The monthly precipitation and temperature rasters, which have 4-kilometer resolution, were downloaded from PRISM Climate Group (2019). Monthly solar radiation was calculated using the input DEM and the Solar Radiation toolset from ArcGIS which approximates the solar load based on terrain, latitude, and time of the year.

To evaluate the ability of CWB metrics to explain tree species distribution, cumulative CWB values from the growing season were used in the modeling framework. For trees in the Eastern United States, the summer months are the most critical for tree growth and, dually, water availability. Summer drought has been linked to patterns of mortality in certain species and recruitment (Berdanier and Clark 2016; Jackson et al. 2009). Additionally, summer drought is the climate variable most correlated with tree growth (Maxwell et al. 2015). Dyer (2019) used the cumulative deficit from June, July, and August from 2012 to investigate the relationship between tree species and summer deficit. CWB metrics were calculated for the study area from the past two decades (2000-2019) and determined 2007 had the largest summer season deficit (183 mm) for this

landscape. Then the Raster Calculator in ArcGIS to calculate cumulative summer CWB metrics for this year.

Statistical Analysis

Generalized linear modeling using logistic regression was used to assess the ability CWB metrics to explain the presence of tree species. The *glm* function in the stats R package was used to create the models (R Core Team 2018). The fitted parameter for each corresponding CWB metric and overall modeling performance in explaining species distribution were compared to commonly used GIS terrain variables. In the analysis framework, there are three model categories: terrain, CWB, and a combination of all the variables from the terrain and CWB categories. The GIS terrain model category includes RSP, SW, solar radiation, slope steepness, TWI, and PC (Figure 3.2). The GIS CWB model category includes PET, AET, deficit, storage, and surplus (Figure 3.3). The third model category is a combination of the variables used in the previous two categories (terrain and CWB). All statistical analyses were done in R version 3.5.1 (R Core Team 2018).

To identify the importance of each variable within each of the three model categories, a model averaging approach was implemented. The *dredge* function in the MuMIn R package (Barton 2019) was used to identify the ranking of variables based on the sum of weights for each species (in all three model categories). The sum of weights for each variable was calculated considering the subset of models with delta AICc < 4.

In addition to the model averaging approach, stepwise AIC was used to identify the top model within each model category for each species. The *stepAIC* function in the MASS R package (Venables and Ripley 2002) was used, with forward and backward

selection, to identify a top model within each of the categories mentioned above (terrain, CWB, and combination) for each of the species. Fit statistics for these top models were calculated, including pseudo R^2 (McFadden value) and area under the receiver operating characteristic curve (AUC). The pseudo R^2 values were calculated using the *nagelkerke* function in the rcompanion R package (Mangiafico 2020). The AUC values were calculated using the *rocplot* function in the Deducer R package (Fellows 2012). The *vuongtest* function in the nonnest2 R package (Merkle and You 2018) was used to formally compare each species' top models selected using StepAIC (from each category: terrain, CWB, and combination) to one another using a non-nested likelihood ratio test. The *vuongtest* function tests the distinguishability of the two models and if one of the two models fit significantly better than the other.

The spatial patterns of predicted distribution maps for each species were created using predictive mapping derived from the three top models (selected from stepwise AIC). A grid of points was created at an interval of 1.5 meters, which was used to extract values from the previously mentioned rasters (with a 9 x 9 cell focal mean). The *predict* function in the stats R package (R Core Team 2018) was used to calculate prediction values for each species using the equations of the top models selected (terrain, CWB, and combination).

RESULTS

Acer rubrum, *Quercus alba*, *Liriodendron tulipifera*, *Quercus montana*, *Fagus grandifolia*, and *Quercus velutina* were the most prevalent species in the 12.5 cm and above DBH size class. Therefore, these six species were used in the modeling framework. For the model averaging approach, the ranking of variables by sum of weights from each model category can be found in Table 3.1. In the terrain model for all six species, RSP appears as the top first or second variable. Solar radiation (either solar or SW) is ranked as the first or second variable for four species in the terrain model. The ranking of variables in the CWB model varies among all species. For the combination model, RSP appears as the first or second variable for all species except for *Quercus velutina*. Storage appears as the first or second variable in the combination model in four species.

Each of the six species studied has different combinations of variables in the top model selected by stepwise AIC. The top models for each species, selected by stepwise AIC, and their corresponding AUC and pseudo R^2 can be found in Table 3.2. All six species have RSP in their top terrain model (Table 3.2). Deficit and PET are the top CWB model using stepwise AIC for *Fagus grandifolia* and *Quercus montana*, while *Acer rubrum* has PET and AET. *Liriodendron tulipifera*'s top CWB model consists of deficit, PET, and storage. *Quercus alba* has PET as its top CWB model, while *Quercus velutina* has storage.

The direction of the relationship between the variables and species is also indicated in Table 3.2. *Acer rubrum*, *Quercus montana*, and *Quercus velutina* have a positive relationship with RSP values. These larger values of RSP indicate that they are found on ridge positions that are generally exposed to xeric conditions with higher solar energy indicated by a positive relationship with SW, solar, PET and lower water

availability shown by the negative relationship with storage (*Quercus montana* and *Quercus velutina*) and the positive relationship with deficit (*Quercus montana*). The more mesic species, including *Fagus grandifolia*, *Liriodendron tulipifera*, and *Quercus alba*, had a negative relationship with RSP, indicating that they are found at lower topographic positions.

The AUC and pseudo R^2 for each species' top terrain model is higher than that of the corresponding CWB model (Table 3.2). The AUC values for each terrain model range from .75 to .95, while the CWB models have AUC values ranging from .65 to .86. The top stepwise combination model for each species has AUC and pseudo R^2 values greater than or equal to the corresponding terrain model and greater than the corresponding CWB model. The AUC scores for the combination model range from .79 to .95.

The non-nested likelihood ratio test formally compares the model performance of the top models for each species (Table 3.3). For *Acer rubrum*, there are no significant differences in fit among the three models. *Fagus grandifolia* has significant results ($p < 0.05$) for each comparison, with the terrain model fitting better than the CWB model and the combination model fitting better than both the terrain and CWB models. *Liriodendron tulipifera* has significant results ($p < 0.01$) for the combination model fitting better than the CWB model, though the terrain model and the combination model were not significantly different. For *Quercus alba*, the terrain model and combination model fit better than the CWB model ($p < 0.05$), however, there is not a significant difference between the terrain model and the combination model. The top terrain and combination models for *Quercus montana* fit better than the CWB model ($p < 0.01$), but there are no

significant differences in fit between the terrain and combination model. *Quercus velutina* does not have significant differences in fit between any of the models.

Prediction maps (Figures 3.2 through 3.7) for the top models of each species' three models (Table 3.2) reveal differences in spatial patterns between the terrain and CWB models. The prediction values indicate the presence probability of the species within a $1/50^{th}$ hectare area. Although there are similarities between the three maps for each species, the terrain and combination maps are more similar for most species, particularly *Fagus grandifolia*, *Quercus alba*, and *Quercus montana*. The CWB models have distinct patterns of aspect differences, while the patterns produced by the terrain models produced more nuanced effects such as differences between topographic positions or combined effects of aspect and topographic position. In general, the prediction values of the terrain and combination maps have higher maximum values, compared to the CWB maps.

DISCUSSION

The results suggest that models with CWB variables alone have weaker fitting power than models with terrain variables in half of the species studied, however, the differences are not substantial. Including CWB variables with terrain variables in the model can improve model performance for some species, but this improvement was significant in only one species studied. In most cases, the terrain variables alone were comparable to the combination model. When using CWB variables, the use of more than one variable is preferred for most species. Additionally, among the terrain variables, RSP is a top-performing variable. Although the model performance between the terrain and CWB variables is not substantial, the spatial prediction patterns produced by the terrain and CWB models differ considerably.

Modeling Tree Species in Dissected Landscapes

Previous studies in similar dissected landscapes have shown the importance of slope aspect in differentiating species distributions and community compositions (Fekedulegn et al. 2003; Hutchins et al. 1976). The results of this study indicate differences in solar radiation, as modified by slope aspect, do differentiate and control species distributions. Variables representing slope aspect or solar radiation were in the top models for most species, however, topographic position seems to have higher importance. Among the GIS terrain variables, RSP ranked as the first or second variable in the model averaging framework for all species and was also included in the top stepwise model of all species. When considering all variables, RSP ranked as the first or second variable for all species except for *Quercus velutina*.

The results suggest that RSP is representing patterns of tree species distribution in this forested watershed. The relationship between topographic position and patterns of microclimate and soil properties may explain why species distributions are partially represented by RSP. Some of these patterns include lower slopes being characterized by cooler temperatures (Franzmeier et al. 1969) and less evaporative demand (Aandahl 1949; Bates 1923), as well as increased soil nutrients and soil moisture, higher pH (Giesler et al. 1998; Kalisz 1986), thicker soil horizons (Cooper 1960), and more organic matter (Aandahl 1949) when compared to higher slope positions.

Although the influences of topographic position on many factors of a landscape's ecology are acknowledged, the way that topographic position is represented in the modeling framework should be considered. Previous studies in the Appalachian region have noted the importance of elevation in capturing species distributions (Day and Monk 1974; Muller 1982; Whittaker 1967). Additionally, Muller (1982) cited the strong relationship between elevation and soil fertility and moisture. How slope position is represented in gradient analysis studies may influence the results, as variables such as elevation or the Topographic Position Index are not comparable across landscapes or in landscapes with variable slope lengths. In these cases, a relativized topographic index could be more appropriate, such as Relative Slope Position used in this study.

With respect to the trends in CWB variables, the top model from the CWB category for most species included two or three CWB variables. Using a single CWB metrics, such as deficit, alone does not appear to explain the most amount of species distribution. Other studies have shown similar approaches, often reporting pairs of CWB metrics, such as AET and deficit, to be useful in differentiating between biomes

(Stephenson 1990) and species (Lutz et al. 2010). The combination of CWB metrics that best describes species distributions will vary among species and locations (Stephenson 1998). Additionally, the distribution of the six species studied in this analysis follows similar patterns of distribution with respect to summer deficit as Dyer (2019) found.

Spatial Patterns of Species Prediction

While the model performance of terrain and CWB variables were not substantially different for all species, the spatial patterns produced by the top model (identified using stepwise AIC) for each model and each species reveal varied prediction patterns (Figures 3.4 through 3.9). The terrain and combination maps (terrain + CWB) generally have higher maximum prediction values for all species, compared to the CWB variables alone. For *Fagus grandifolia*, *Quercus alba*, and *Quercus montana* the combination and terrain models fit significantly better than the CWB model (as reported by the non-nested likelihood ratio test), which is reflected in the spatial patterns of prediction values. The patterns of prediction for the terrain and combination maps are more nuanced when compared to CWB. Many of maps, especially those produced by the terrain and combination models, reflect patterns of species distribution described by other studies in this region (Braun 1942; Fralish et al. 1993; Muller 1982).

The six tree species included in the analysis represent varied distributions within this watershed, as well as varied specificities for site type, as reflected by the prediction maps. *Acer rubrum* (Figure 3.4) has high prediction values for much of the study area, especially on ridges and the southwest-facing aspect. Other studies found similar patterns of distribution, noting that *Acer rubrum*, which is present in the most plots for the size

class studied, can thrive on a wider range of soil textures, pH, moisture, and elevation compared to other tree species (Iverson et al. 1997).

Fagus grandifolia (Figure 3.5) has the highest prediction values in valley slope positions, northeast-facing aspect, and sheltered locations, which is a similar distribution pattern of that described by Fralish et al. (1993) and Muller (1982). The terrain and combination maps reflect these distributions, but the CWB prediction map does not show these nuanced patterns, rather it reflects lower to moderate prediction values on the northeast-facing slope (Figure 3.5). *Liriodendron tulipifera* (Figure 3.6) has higher prediction values across mesic sites, like *Fagus grandifolia*, but with a wider topographic position range. The patterns created by the terrain and combination models show more nuanced patterns, especially favoring the northeast-facing slope and cove positions. Though the CWB map illustrates similar patterns, the prediction power is lower than that of the other two maps.

The prediction patterns of *Quercus alba* (Figure 3.7) show a preference for middle to lower slope positions on most aspects except for the northeast/north-facing aspects. Fralish et al. (1993) found *Quercus alba* to be on west, southwest, and southeast slopes, primarily at middle slope elevations, which is illustrated in the prediction maps. Although the slope differences are reflected by all three model categories, the prediction differences between slope positions are more evident in the terrain and combination maps. *Quercus montana* (Figure 3.8) has high prediction values for ridge slope positions in all three maps, reflecting the patterns of RSP and TWI which were selected in the top model, with higher prediction values in the terrain and combination models. Day and Monk (1974) noted the only species positively correlated with elevation was *Quercus*

montana (= *Quercus prinus*), which found at the extremes of the elevation gradient. *Quercus velutina* (Figure 3.9) has generally lower prediction values overall, with higher prediction values on ridges as well.

Topography modifies the distribution of plant relevant resources and influences tree species distribution which is evident in the model selection process and, subsequently, reflected by the pattern of species distribution in our study and previous studies (Braun 1950; Day and Monk 1974; Fralish et al. 1993; Hutchins et al. 1976; Whittaker 1956). The prediction maps produced by the CWB models reflect the dominant influence of solar radiation and aspect, however, the influences of topographic position on water availability patterns are less evident. CWB variables, especially storage and other variables that implement available water capacity data from the NRCS database, show strong patterns of the northeast and southwest-facing aspects, and the ridge topographic position. The coarseness of the NRCS SSURGO data results in a spatial pattern of CWB variables, such as storage, that can be categorical in. Using soil data that is fine-scale and more representative of the study area would likely result in different spatial patterns, however, if ease of use is of interest for the user of this CWB toolset, relying on user-supplied fine-scale soil data may not be the best solution. Moore et al. (1993) noted that the resolution of soil maps is often too coarse for the use in detailed environmental modeling, but the integration of terrain variables with this soil data may mitigate this issue. In comparison to the spatial patterns produced by the CWB models, patterns of topographic position are evident in most of the terrain and combination (terrain + CWB) maps.

Limitations and Future Work

The GIS-derived terrain variables used in this study were highly effective at explaining the distribution of species in this watershed. These terrain variables are, however, static variables that will not reflect climate changes throughout time. Therefore, when studying climate change and how species, populations, and even communities will shift under evolving conditions, the use of temporally dynamic climate variables that reflect these changes is important. The integration of more terrain variables, such as RSP and slope steepness, into how available water is calculated in the GIS CWB toolset can potentially increase its applicability in dissected landscapes.

In this study cumulative 2007 summer season values from the CWB toolset output were used to investigate the toolset's explanatory and predictive power. The trees used as response variables in this study were greater than or equal to 12.5 cm in DBH, meaning that many trees were established prior to the timeframe investigated. Though they were established under different conditions from the dry season of 2007, the CWB toolset likely produces similar spatial patterns of deficit/PET/storage despite the exact climatic conditions. Different CWB metrics, either monthly or cumulative, could be investigated to see if the same trends are detected. The vegetation data used is another factor that can be changed, such as different size classes of trees and herbaceous plants, which are representative of more recent climate conditions.

Future studies can investigate the landscape scale spatial distribution patterns of predicted CWB metrics and the associated tree species distributions in other dissected landscapes. Different ecology, land-use history, terrain, and influential factors will control species distribution, and the results from this watershed may not apply to other locations. Future work that compares CWB prediction power in different landscape

settings is warranted to enhance our understanding of the strengths and weaknesses of this approach in different areas.

CONCLUSION

The results suggest that the model performance of terrain and CWB variables in predicting tree species distribution in this central Appalachian watershed are significantly different for some species. Conversely, including CWB variables in models with terrain variables can be advantageous. In respect to CWB variable performance, the distribution of species in our study area is best explained by at least two CWB variables, rather than solely deficit. Aspect and topographic position, which are widely recognized as two factors controlling species distribution, were well represented by the variables included in this analysis. RSP, representing the topographic position, performed well across most species, while the variables best representing aspect/solar radiation varied.

CWB addresses the need to move toward dynamic plant relevant variables in the future as climate change progresses and plant distributions change. The current GIS iteration of the CWB does not, however, perform better than GIS-derived terrain variables in predicting tree species presence. When using CWB variables to study tree species distributions, the inclusion of terrain variables such as topographic position may increase the explanation power of the model as the effects of topographic position are not currently included in the CWB toolset.

Table 3.1 Ranking of predictor variables by sum of weights for each species within terrain, Climate Water Balance (CWB), and Combination (Terrain and CWB) variable categories.

Species	Model	Ranking*	Sum of Weights
Acer rubrum	Terrain	RSP SW Solar TWI PC Slope	1.00 0.76 0.38 0.29 0.27 0.19
	CWB	Storage Deficit PET AET	0.55 0.47 0.43 0.43
	Combination	RSP SW Solar PC TWI Deficit	1.00 0.58 0.23 0.23 0.21 0.20
Fagus grandifolia	Terrain	RSP Solar SW PC Slope TWI	1.00 0.62 0.49 0.34 0.24 0.20
	CWB	AET PET Deficit Storage	0.72 0.62 0.62 0.32
	Combination	RSP Storage AET Deficit PET SW	1.00 1.00 0.66 0.65 0.60 0.33
Liriodendron tulipifera	Terrain	Slope RSP SW TWI Solar PC	1.00 0.78 0.67 0.54 0.41 0.22
	CWB	Deficit PET AET Storage	0.71 0.63 0.60 0.52
	Combination	Storage RSP Slope Solar PET Deficit	0.89 0.85 0.79 0.62 0.50 0.49
Quercus alba	Terrain	Solar RSP TWI SW Slope PC	0.96 0.70 0.69 0.31 0.25 0.22
	CWB	PET Deficit AET Storage	0.57 0.49 0.48 0.38
	Combination	RSP Storage TWI Deficit PET Solar	0.97 0.62 0.42 0.31 0.19 0.17
Quercus montana	Terrain	RSP TWI SW PC Solar Slope	1.00 0.75 0.54 0.46 0.33 0.21
	CWB	AET PET Deficit Storage	0.76 0.53 0.53 0.48
	Combination	RSP TWI SW PC AET Storage	1.00 0.79 0.45 0.42 0.34 0.31
Quercus velutina	Terrain	Solar RSP SW PC Slope TWI	1.00 0.51 0.47 0.41 0.39 0.35
	CWB	Storage Deficit PET AET	1.00 0.33 0.33 0.32
	Combination	Storage Slope SW Solar Deficit PC	0.84 0.54 0.45 0.35 0.34 0.28

Table 3.1 (continued)
* Abbreviated variable names are as follows: relative slope position (RSP), southwestness (SW), plan curvature (PC), slope steepness (Slope), solar radiation (Solar), topographic wetness index (TWI), CWB storage (Storage), potential evapotranspiration (PET), actual evapotranspiration (AET), CWB deficit (Deficit). Only the top six variables are shown in the Combination category.

Table 3.2 Terrain, Climate Water Balance (CWB), and Combination (Terrain and CWB variables) models selected using stepwise AIC for each tree species.

Species	Model	Top Stepwise Model*	AUC	Pseudo R^2
Acer rubrum	Terrain	RSP + SW	0.78	0.17
	CWB	PET + AET	0.74	0.12
	Combination	RSP + SW + PC + Deficit + PET + AET + TWI	0.79	0.21
Fagus grandifolia	Terrain	RSP + SW	0.85	0.34
	CWB	Deficit + PET	0.70	0.24
	Combination	RSP + PET + AET + Storage	0.90	0.43
Liriodendron tulipifera	Terrain	Slope + RSP + SW	0.82	0.26
	CWB	PET + AET + Storage	0.76	0.19
	Combination	Slope + Solar + Storage + RSP + AET	0.85	0.32
Quercus alba	Terrain	Solar + TWI + RSP	0.75	0.15
	CWB	PET	0.65	0.06
	Combination	PET + RSP + TWI	0.75	0.15
Quercus montana	Terrain	RSP + TWI + SW	0.95	0.58
	CWB	Deficit + PET	0.86	0.32
	Combination	RSP + TWI + Storage	0.95	0.58
Quercus velutina	Terrain	Solar + RSP + Slope + SW	0.81	0.22
	CWB	Storage	0.78	0.20
	Combination	Storage + Slope + PC	0.82	0.23

Table 3.2 (continued)
* Abbreviated variable names are as follows: relative slope position (RSP), southwestness (SW), plan curvature (PC), slope steepness (Slope), solar radiation (Solar), topographic wetness index (TWI), CWB storage (Storage), potential evapotranspiration (PET), actual evapotranspiration (AET), CWB deficit (Deficit). Variables are listed in order of increasing p-values. Variables that are underlined have a negative relationship with the species' presence. The pseudo R^2 values reported are the McFadden pseudo R^2 values

Table 3.3 Non-nested likelihood ratio test results for top models selected by stepwise AIC in three GIS variable categories: Terrain, Climate Water Balance (CWB), and Combination.

Species	Non-nested Likelihood Ratio Test	
Acer rubrum	Terrain fits better than CWB	p = 0.112
	Combination fits better than CWB	p = 0.061
	Combination fits better than Terrain	p = 0.205
Fagus grandifolia	Terrain fits better than CWB	**p = 0.038**
	Combination fits better than CWB	**p < 0.001**
	Combination fits better than Terrain	**p = 0.030**
Liriodendron tulipifera	Terrain fits better than CWB	p = 0.101
	Combination fits better than CWB	**p = 0.009**
	Combination fits better than Terrain	p = 0.061
Quercus alba	Terrain fits better than CWB	**p = 0.036**
	Combination fits better than CWB	**p = 0.030**
	Combination fits better than Terrain	p = 0.367
Quercus montana	Terrain fits better than CWB	**p = 0.002**
	Combination fits better than CWB	**p = 0.001**
	Terrain fits better than Combination	p = 0.476
Quercus velutina	Terrain fits better than CWB	p = 0.285
	Combination fits better than CWB	p = 0.131
	Combination fits better than Terrain	p = 0.389

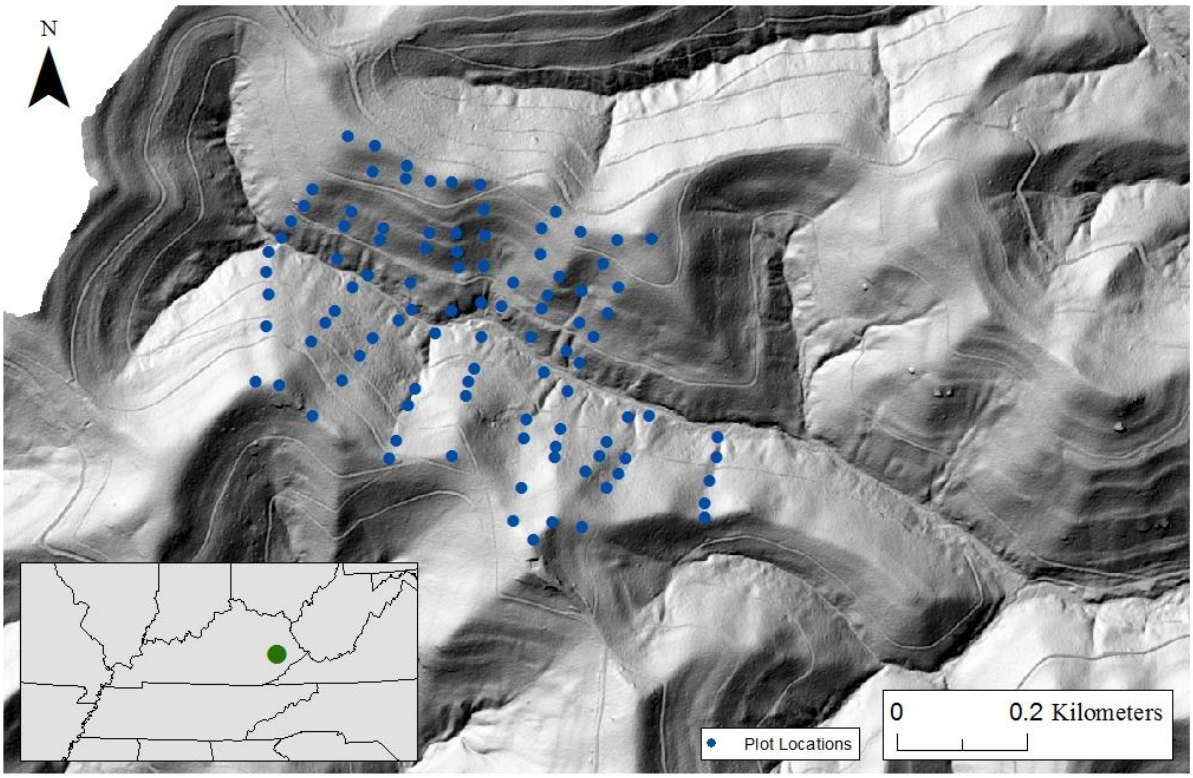

Figure 3.1 Plot locations in Little Millseat watershed located in Kentucky, USA

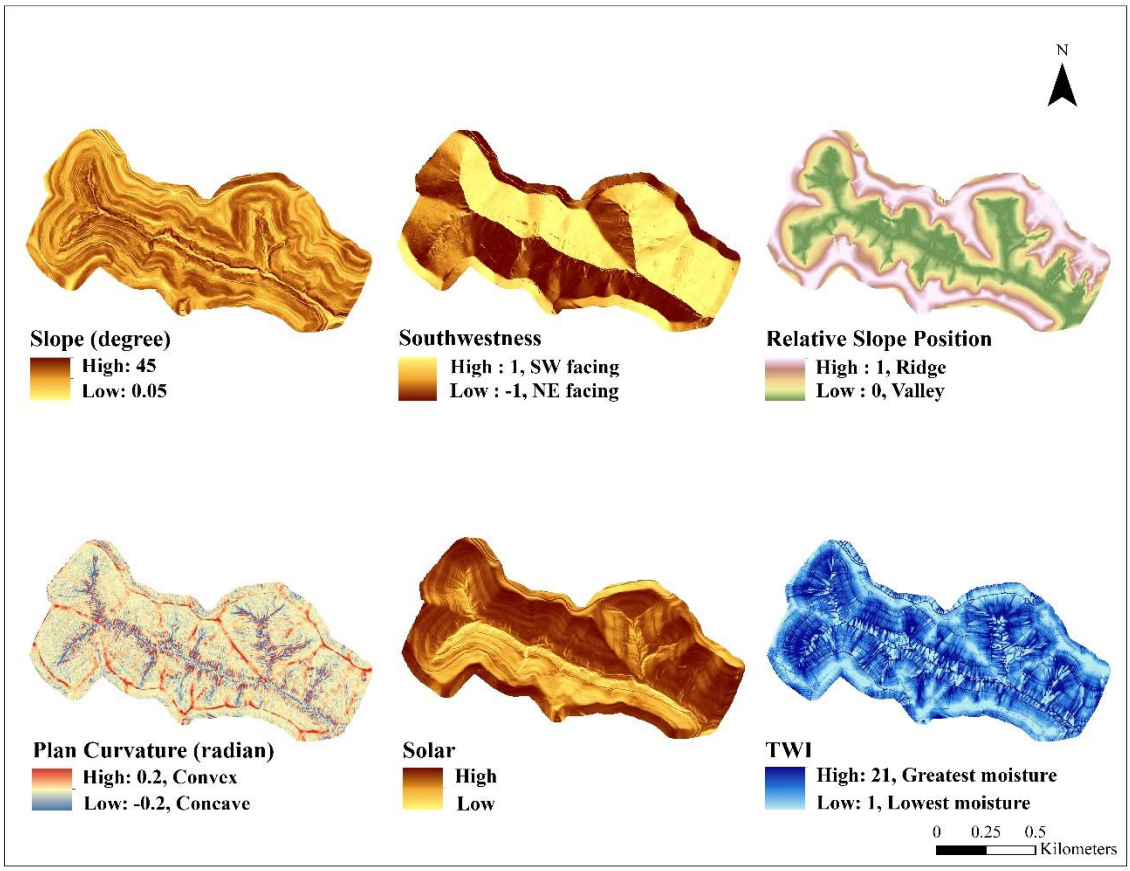

Figure 3.2 GIS terrain variables used in the terrain category, from left to right, top to bottom: Slope, Southwestness, Relative Slope Position, Plan Curvature, Solar, and Topographic Wetness Index (TWI).

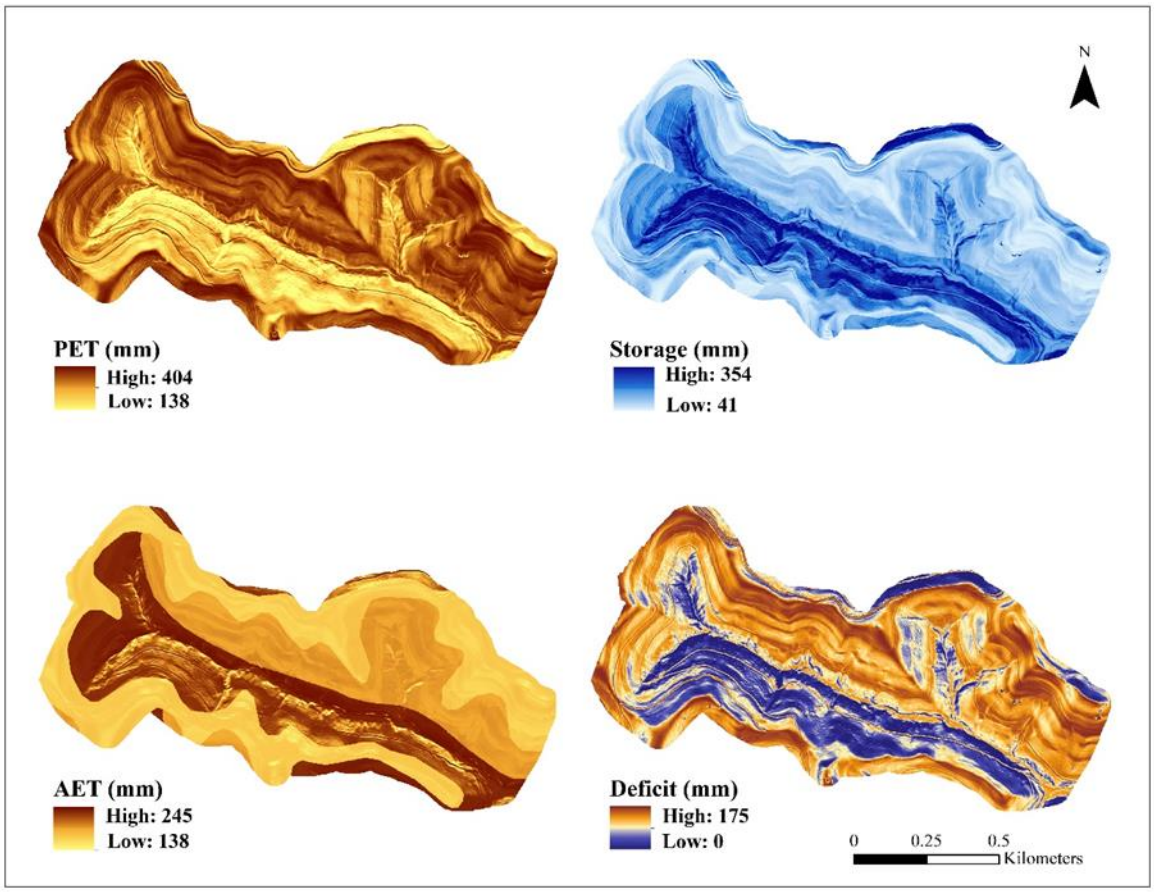

Figure 3.3 GIS Climate Water Balance (CWB) variables used in the CWB category, from left to right, top to bottom: PET, Storage, AET, and Deficit. CWB variables reflect cumulative calculations for June, July, and August of 2007.

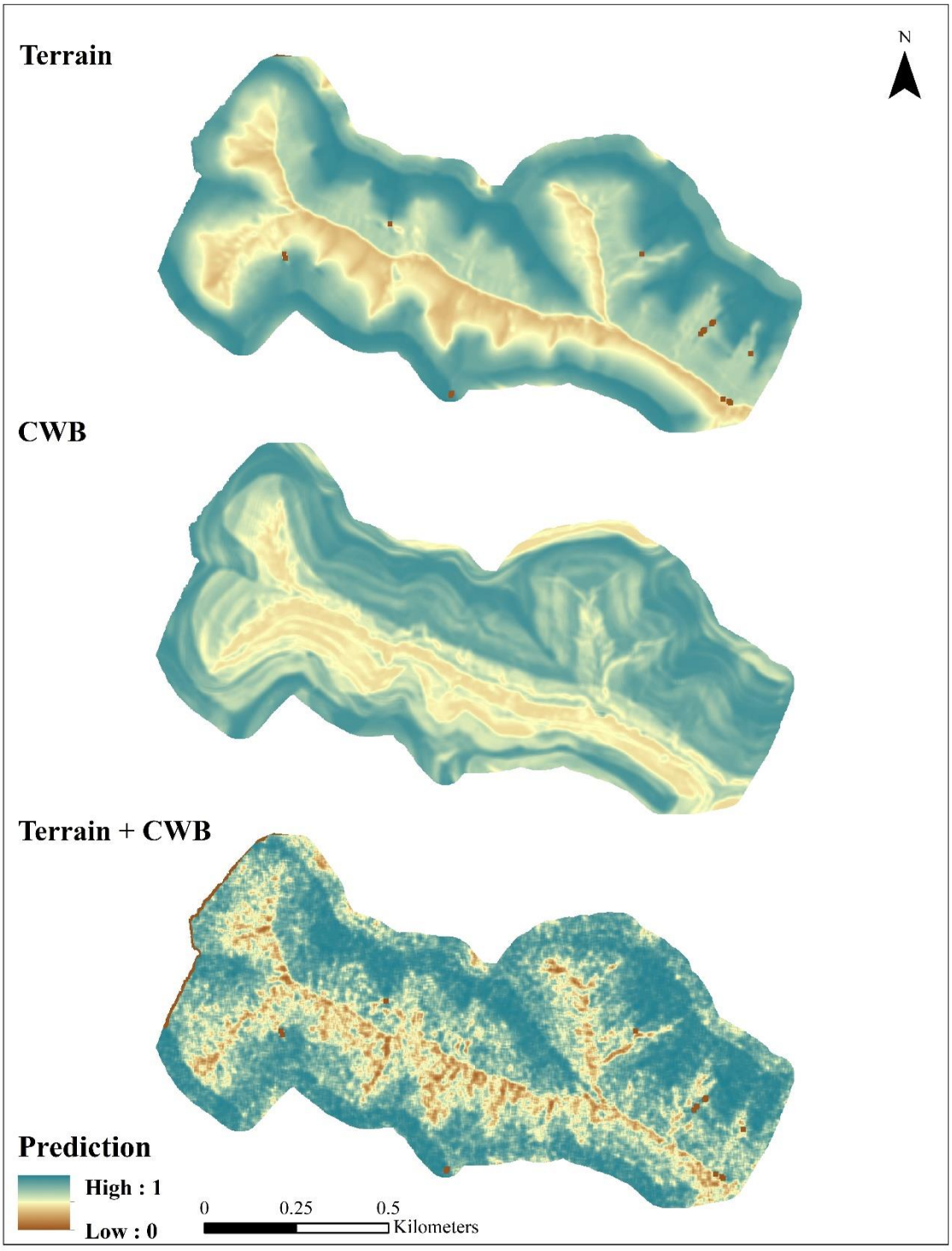

Figure 3.4 *Acer rubrum* prediction maps for each top model selected by stepwise AIC.

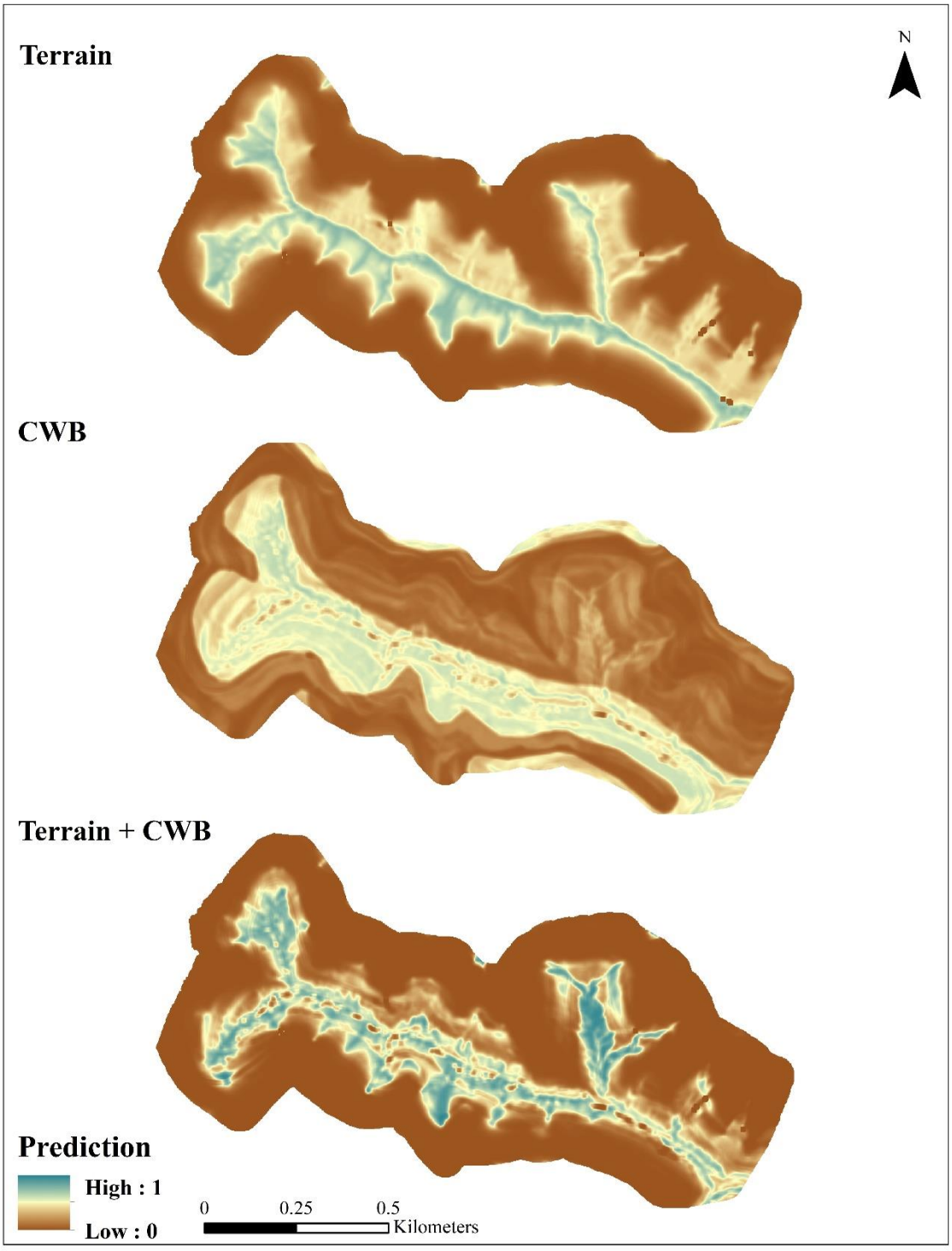

Figure 3.5 *Fagus grandifolia* prediction maps for each top model selected by stepwise AIC.

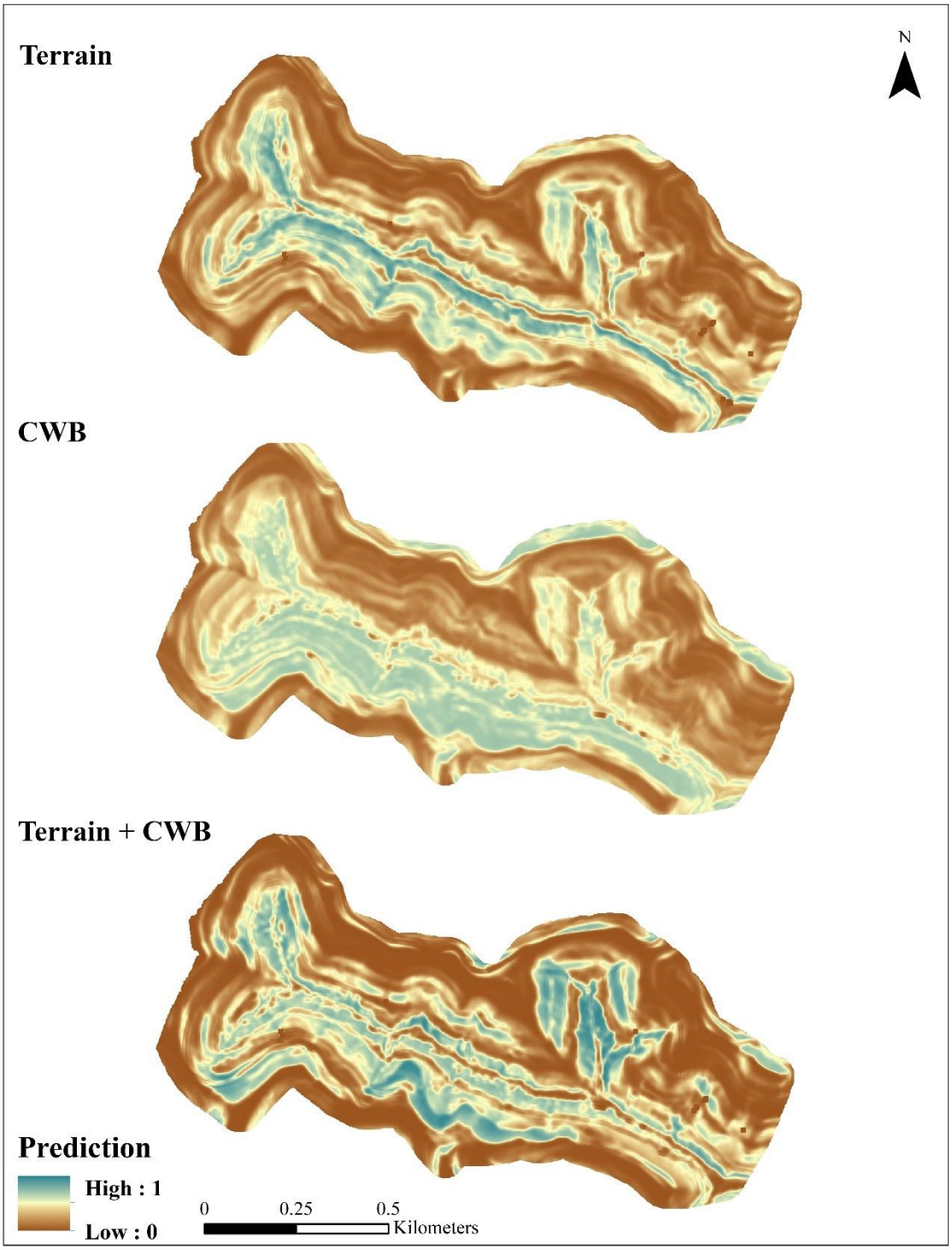

Figure 3.6 *Liriodendron tulipifera* prediction maps for each top model selected by stepwise AIC.

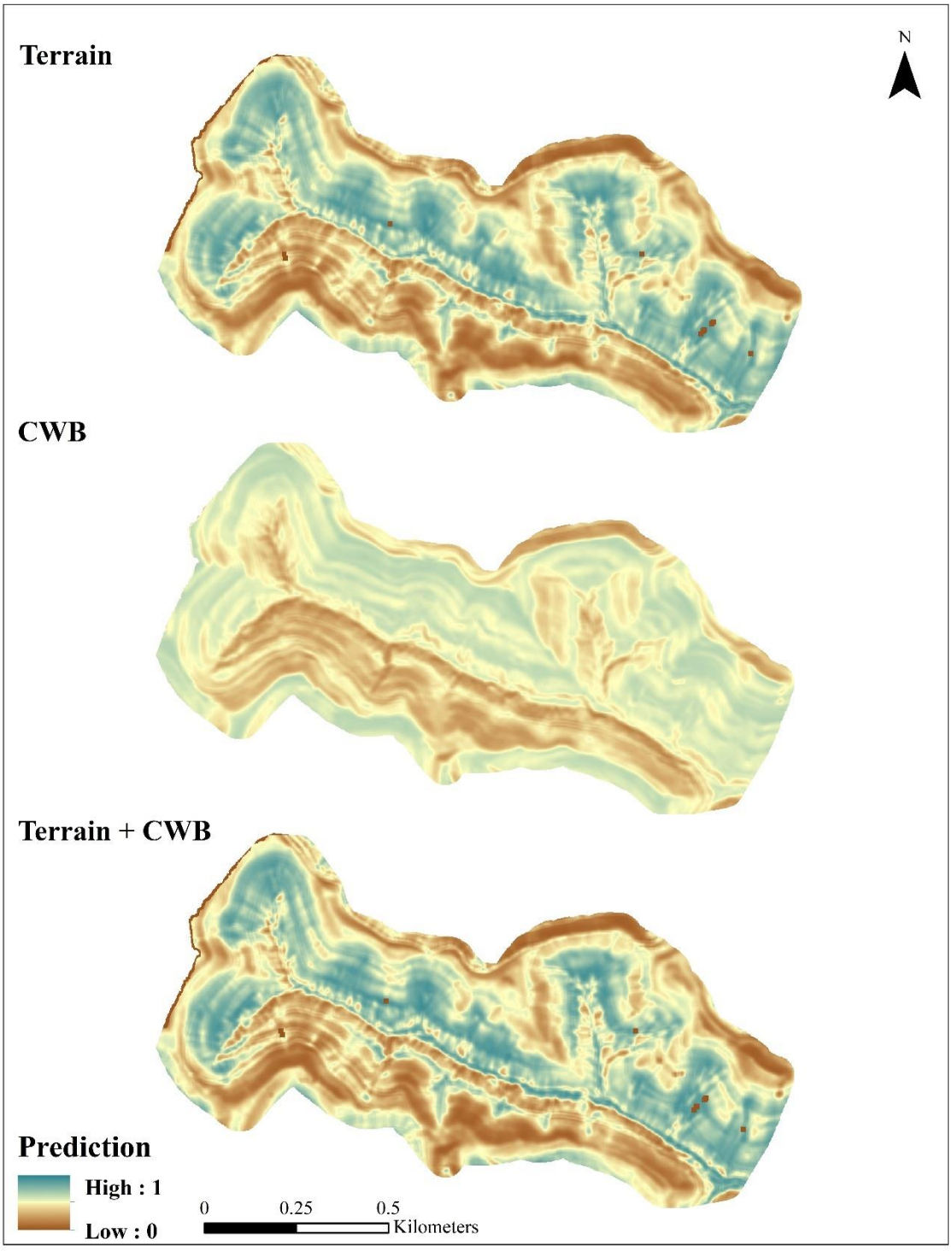

Figure 3.7 *Quercus alba* prediction maps for each top model selected by stepwise AIC.

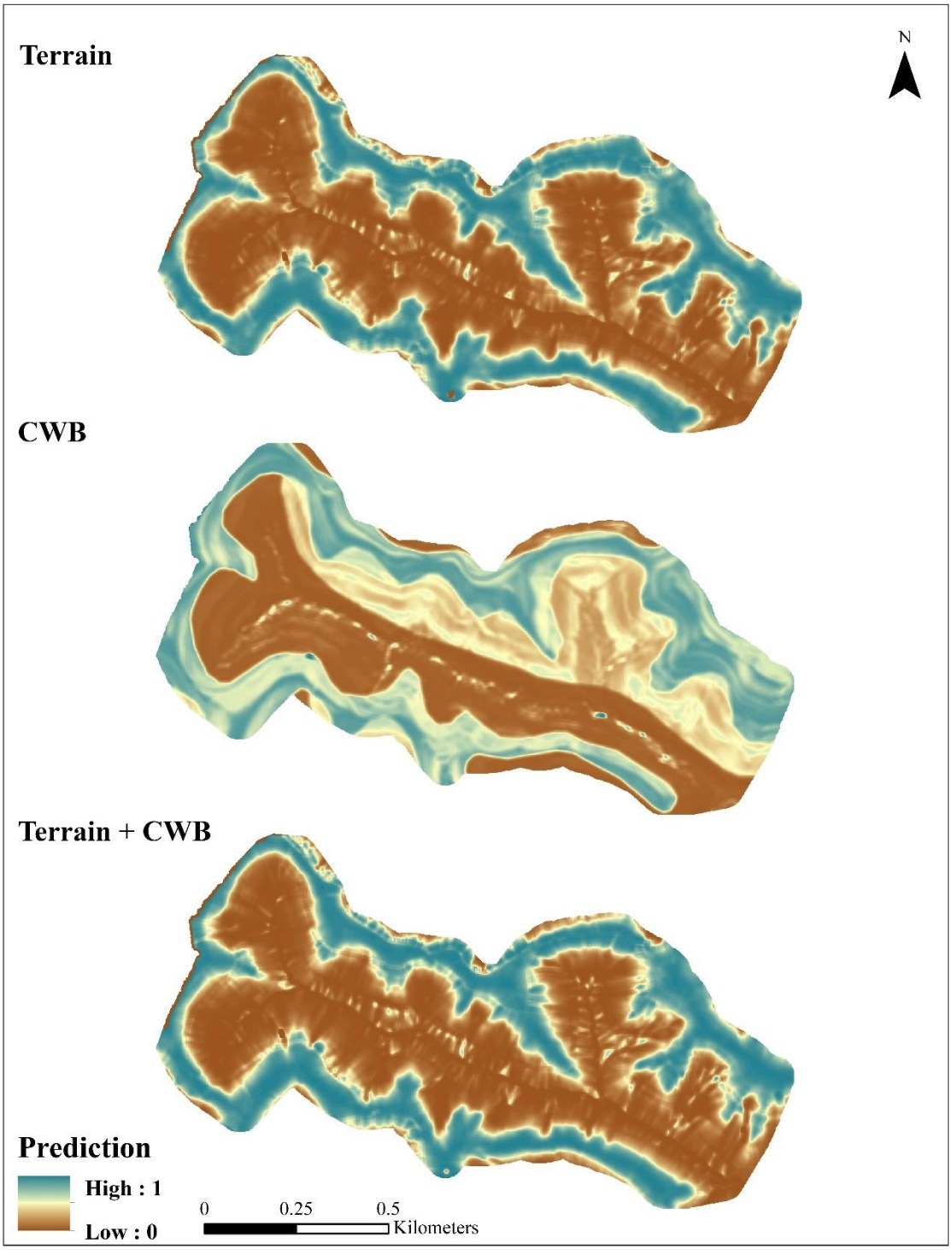

Figure 3.8 *Quercus montana* prediction maps for each top model selected by stepwise AIC.

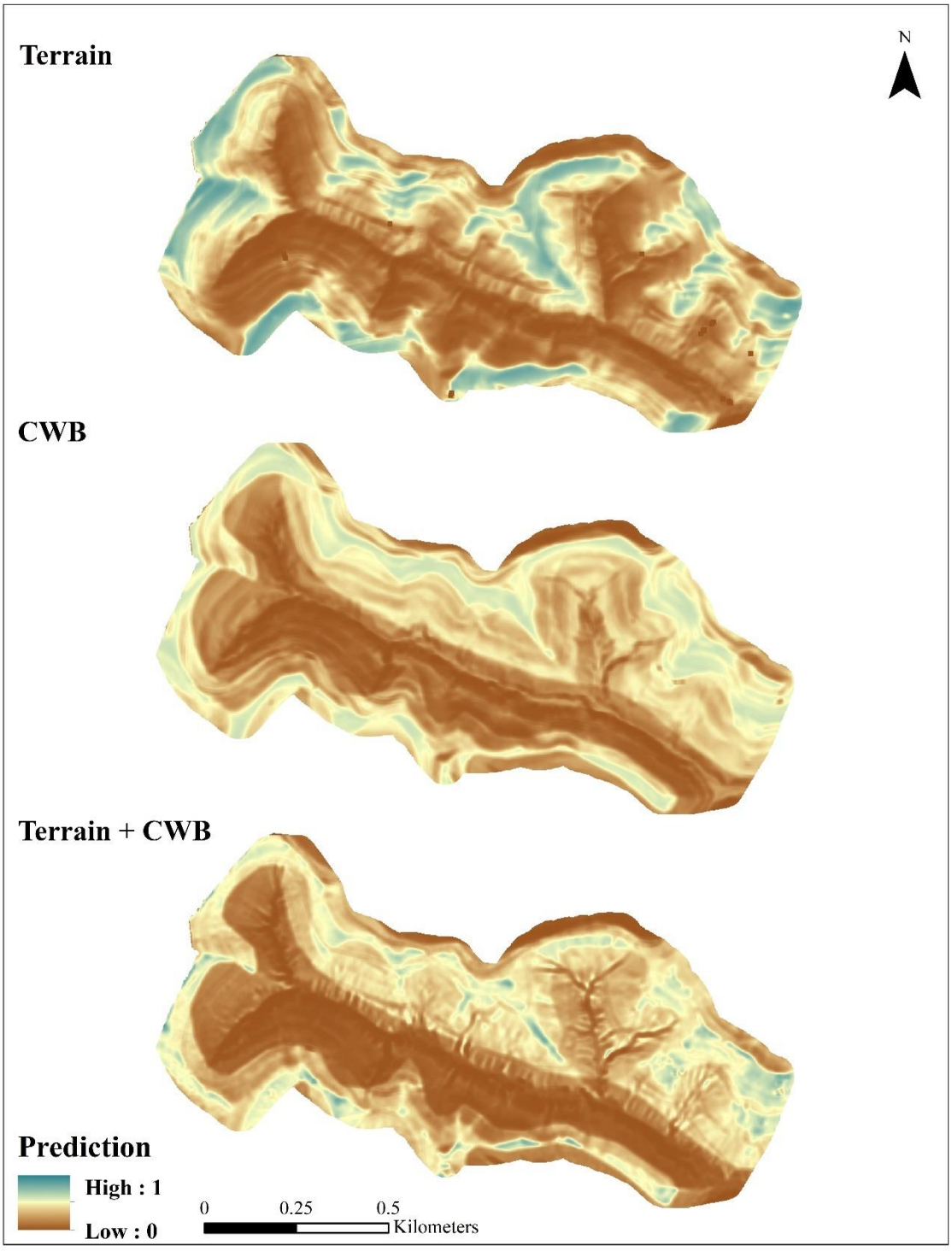

Figure 3.9 *Quercus velutina* prediction maps for each top model selected by stepwise AIC.

CHAPTER 4 CONCLUSION

The results from this thesis suggest the current CWB toolset variables alone do not perform better than GIS-derived terrain variables in explaining soil moisture and tree species distribution in a dissected watershed in the Cumberland Plateau. However, the differences in model performance between the terrain and CWB models in explaining soil moisture and half of the tree species studied are not significant. The other species did show a significant difference between the performance of terrain and CWB models, with the terrain models better fitting the data. For both soil moisture and species distributions, the results suggest that the inclusion of terrain variables with CWB variables improves performance in comparison to CWB variables alone. Conversely, in most cases, the model performance of the terrain variables alone is comparable to that of the combined model. In assessing the spatial patterns produced by terrain and CWB models, the results suggest that the tree species prediction patterns produced by of terrain and CWB variables to differ substantially.

The long-understood concept that terrain, including slope aspect and topographic position, shapes the ecology of a landscape is supported by the results of this study. For soil moisture, CWB storage is the top CWB variable, while among the terrain variables, relative slope position (RSP), slope steepness, and a measure of solar radiation (southwestness (SW) or solar) are important variables. In explaining tree species distribution, the top CWB variables for each species varies, however, most of the species studied include two or three variables to describe the species' distribution. As found with soil moisture, among the GIS-derived terrain variables, RSP is an important variable in explaining tree species distribution, along with measures of solar radiation (SW or solar).

As the effects of topographic position are not currently included in how the CWB toolset calculates water available to the site, the results indicate that RSP captures ecological processes not represented by the CWB toolset variables. In dissected landscapes, topographic position is associated with many ecological patterns including soil properties, drainage, site exposure to solar radiation, and vegetation distribution. The inclusion of topographic position into the CWB toolset, such as by using the terrain variable RSP, may capture the influences of topography on patterns of soil moisture and tree species distribution. The easily derived terrain variables used in this study capture fine-scale terrain patterns of ecological processes across a landscape, however, they do not capture the temporal dynamics of resources pertinent to plants. Temporally dynamic variables, such as CWB, present monthly and annual patterns of available moisture in a way that will reflect changes in climate. Integrating topographic position into the current CWB toolset, or in tandem with CWB metrics, may prove to capture spatial distributions of both moisture availability and tree species.

REFERENCES

Aandahl AR (1949) The characterization of slope positions and their influence on the total nitrogen content of a few virgin soils of western Iowa. Soil Science Society of America Journal 13(C):449-454

Abnee AC, Thompson JA, Kolka RK, D'Angelo EM, Coyne MS (2004) Landscape influences on potential soil respiration rates in a forested watershed of southeastern Kentucky. Environmental Management 33(1):S160-S167

Allen CD, Macalady AK, Chenchouni H et al (2010) A global overview of drought and heat-induced tree mortality reveals emerging climate change risks for forests. Forest ecology and management 259(4):660-684

Bailey RG (2009) Ecosystem geography: from ecoregions to sites. Springer Science & Business Media

Barton K (2019) MuMIn: Multi-Model Inference. R package version 1.43.6. https://CRAN.R-project.org/package=MuMIn

Bates CG (1923) The transect of a mountain valley. Ecology 4(1):54-62

Berdanier AB, Clark JS (2016) Multiyear drought-induced morbidity preceding tree death in southeastern US forests. Ecological Applications 26(1):17-23

Berg B, Berg M, Bottner P et al (1993) Litter mass loss rates in pine forests of Europe and Eastern United States: some relationships with climate and litter quality. Biogeochemistry 20(3):127-159

Bertin RI (2008) Plant phenology and distribution in relation to recent climate change. The Journal of the Torrey Botanical Society 135(1):126-147

Beven KJ, Kirkby MJ (1979) A physically based, variable contributing area model of basin hydrology. Hydrological Sciences Journal 24(1):43-69

Boerner RJ (2006) Unraveling the Gordian Knot: interactions among vegetation, topography, and soil properties in the central and southern Appalachians. The Journal of the Torrey Botanical Society 133(2):321-361

Boisvenue C, Running SW (2006) Impacts of climate change on natural forest productivity–evidence since the middle of the 20th century. Global Change Biology 12(5):862-882

Braun E (1950) Eastern deciduous forests of North America. Blakiston, Philadelphia

Braun EL (1942) Forests of the Cumberland Mountains. Ecological Monographs 12(4):413-447

Budyko MI, Miller DH, Miller DH (1974) Climate and life. Academic press New York

Burt R, Reinsch T, Miller W (1993) A micro-pipette method for water dispersible clay. Communications in soil science and plant analysis 24(19-20):2531-2544

Burt T, Butcher D (1985) Topographic controls of soil moisture distributions. Journal of Soil Science 36(3):469-486

Chen I-C, Hill JK, Ohlemüller R, Roy DB, Thomas CD (2011) Rapid range shifts of species associated with high levels of climate warming. Science 333(6045):1024-1026

Chirico GB, Grayson RB, Western AW (2003) A downward approach to identifying the structure and parameters of a process-based model for a small experimental catchment. Hydrological Processes 17(11):2239-2258

Clark JS (1990) Landscape interactions among nitrogen mineralization, species composition, and long-term fire frequency. Biogeochemistry 11(1):1-22

Cleland EE, Chuine I, Menzel A, Mooney HA, Schwartz MD (2007) Shifting plant phenology in response to global change. Trends in Ecology & Evolution 22(7):357-365

Collins M, Knutti R, Arblaster J et al (2013) Long-term climate change: projections, commitments and irreversibility. Climate Change 2013-The Physical Science Basis: Contribution of Working Group I to the Fifth Assessment Report of the Intergovernmental Panel on Climate Change. Cambridge University Press, pp. 1029-1136

Conrad O, Bechtel B, Bock M et al (2015) System for Automated Geoscientific Analyses (SAGA) v. 2.1.4. Geosci. Model Dev. 8(7):1991-2007

Cooper AW (1960) An example of the role of microclimate in soil genesis. Soil Science 90(2):109-120

Corlett RT, Westcott DA (2013) Will plant movements keep up with climate change? Trends in ecology & evolution 28(8):482-488

Cremeans D (1992) Aspect and slope position effects on moisture regime and properties of forest soils in eastern Kentucky. In: Kalisz P. J. (ed). ProQuest Dissertations Publishing,

Crimmins SM, Dobrowski SZ, Greenberg JA, Abatzoglou JT, Mynsberge AR (2011) Changes in climatic water balance drive downhill shifts in plant species' optimum elevations. Science 331(6015):324-327

Currie DJ (1991) Energy and large-scale patterns of animal-and plant-species richness. The American Naturalist 137(1):27-49

Currie DJ, Paquin V (1987) Large-scale biogeographical patterns of species richness of trees. Nature 329(6137):326-327

Davis MB, Shaw RG (2001) Range shifts and adaptive responses to Quaternary climate change. Science 292(5517):673-679

Day FP, Monk CD (1974) Vegetation patterns on a southern Appalachian watershed. Ecology 55(5):1064-1074

Dilts TE (2015) Topography Tools for ArcGIS 10.1. University of Nevada Reno. Available at: http://www.arcgis.com/home/item.html?id=b13b3b40fa3c43d4a23a1a09c5fe96b9

Doi H, Katano I (2008) Phenological timings of leaf budburst with climate change in Japan. Agricultural and forest meteorology 148(3):512-516

Dyer JM (2009) Assessing topographic patterns in moisture use and stress using a water balance approach. Landscape Ecology 24(3):391-403

Dyer JM (2019) A GIS-Based Water Balance Approach Using a LiDAR-Derived DEM Captures Fine-Scale Vegetation Patterns. Remote Sensing 11(20):2385

Dyer ML, Meentemeyer V, Berg B (1990) Apparent controls of mass loss rate of leaf litter on a regional scale: litter quality vs. climate. Scandinavian Journal of Forest Research 5(1-4):311-323

Eckert AJ, Eckert ML (2007) Environmental and ecological effects on size class distributions of Foxtail Pine (Pinus balfouriana, Pinaceae) in the Klamath Mountains, California. Madroño:117-125

ESRI (2011) ArcGIS Desktop: Release 10. Redlands, CA: Environmental Systems Research Institute.

Famiglietti JS, Rudnicki J, Rodell M (1998) Variability in surface moisture content along a hillslope transect: Rattlesnake Hill, Texas. Journal of Hydrology 210(1-4):259-281

Fekedulegn D, Hicks Jr RR, Colbert J (2003) Influence of topographic aspect, precipitation and drought on radial growth of four major tree species in an Appalachian watershed. Forest ecology and management 177(1-3):409-425

Fellows I (2012) Deducer: A Data Analysis GUI for R. Journal of Statistical Software, 49(8), 1-15. URL http://www.jstatsoft.org/v49/i08/

Fisher R, Binkley D (2000) Ecology and Management of Forest Soils. John Willey & Sons

Florinsky IV, Eilers RG, Manning G, Fuller L (2002) Prediction of soil properties by digital terrain modelling. Environmental Modelling & Software 17(3):295-311

Fox J, Weisberg S (2011) An R Companion to Applied Regression. Sage, Thousand Oaks CA, 2nd edition. URL http://z.umn.edu/carbook.

Fralish JS, Franklin SB, Robertson PA, Kettler SM, Crooks FB (1993) An ordination of compositionally stable and unstable forest communities at Land Between the Lakes, Kentucky and Tennessee. Fifty years of Wisconsin plant ecology. Madison, WI: Wisconsin Academy of Sciences, Arts and Letters:247-267

Frank DA, Inouye RS (1994) Temporal variation in actual evapotranspiration of terrestrial ecosystems: patterns and ecological implications. Journal of Biogeography:401-411

Franklin S, Fralish J, Close D (2002) History, classification, and effects of disturbance on forest communities in Land Between The Lakes. Land Between The Lakes, Kentucky and Tennessee: four decades of Tennessee Valley Authority stewardship. Center For Field Biology, Austin Peay State University, Clarksville, Tennessee:175-199

Franklin SB, Robertson PA, Fralish JS, Kettler SM (1993) Overstory vegetation and successional trends of Land Between The Lakes, USA. Journal of Vegetation Science 4(4):509-520

Franzmeier DP, Pedersen EJ, Longwell TJ, Byrne JG, Losche CK (1969) Properties of Some Soils in the Cumberland Plateau as Related to Slope Aspect and Position1. Soil Science Society of America Journal 33(5):755

Giesler R, Högberg M, Högberg P (1998) Soil chemistry and plants in Fennoscandian boreal forest as exemplified by a local gradient. Ecology 79(1):119-137

Gottfried M, Pauli H, Futschik A et al (2012) Continent-wide response of mountain vegetation to climate change. Nature climate change 2(2):111-115

Hannah L, Flint L, Syphard AD, Moritz MA, Buckley LB, McCullough IM (2014) Fine-grain modeling of species' response to climate change: Holdouts, stepping-stones, and microrefugia. Trends in Ecology & Evolution 29(7):390-397

Hinrichs EN (1978) Geologic Map of the Noble Quadrangle, Eastern Kentucky: Geologic Quadrangle 1476.

Holdridge LR (1967) Life zone ecology. Life zone ecology.(rev. ed.))

Hutchins RB, Blevins RL, Hill JD, White EH (1976) The influence of soils and microclimate on vegetation of forested slopes in eastern Kentucky. Soil Science 121(4):234-241

Iverson LR, Dale ME, Scott CT, Prasad A (1997) A GIS-derivedintegrated moisture index to predict forest composition and productivity of Ohio forest (USA). Landscape Ecology 12(5):331-348

Iverson LR, Prasad AM, Rebbeck JA (2004) comparison of the integrated moisture index and the topographic wetness index as related to two years of soil moisture monitoring in Zaleski State Forest, Ohio. In: In: Yaussy, Daniel A.; Hix, David M.; Long, Robert P.; Goebel, P. Charles, eds. Proceedings, 14th Central Hardwood Forest Conference; 2004 March 16-19; Wooster, OH. Gen. Tech. Rep. NE-316. Newtown Square, PA: US Department of Agriculture, Forest Service, Northeastern Research Station: 515-517, 2004a.

Iverson LR, Schwartz MW, Prasad AM (2004b) How fast and far might tree species migrate in the eastern United States due to climate change? Global Ecology and Biogeography 13(3):209-219

Jackson ST, Betancourt JL, Booth RK, Gray ST (2009) Ecology and the ratchet of events: climate variability, niche dimensions, and species distributions. Proceedings of the National Academy of Sciences 106(Supplement 2):19685-19692

Jenny H (1980) The soil resource : origin and behavior. New York : Springer-Verlag, New York

Jensen ME, Allen RG Evaporation, evapotranspiration, and irrigation water requirements. In, 2016. American Society of Civil Engineers,

Jump AS, Penuelas J (2005) Running to stand still: adaptation and the response of plants to rapid climate change. Ecology letters 8(9):1010-1020

Kalisz PJ (1986) Soil properties of steep Appalachian old fields. Ecology 67(4):1011-1023

Kelly AE, Goulden ML (2008) Rapid shifts in plant distribution with recent climate change. Proceedings of the National Academy of Sciences

Kentucky Mesonet (2019) Western Kentucky University. Monthly Climatological Summary for Quicksand Station in Breathitt County, Kentucky. Accessed January 2020.

Keppel G, Van Niel KP, Wardell-Johnson GW et al (2012) Refugia: Identifying and understanding safe havens for biodiversity under climate change. Global Ecology and Biogeography 21(4):393-404

Lenoir J, Hattab T, Pierre G (2017) Climatic microrefugia under anthropogenic climate change: implications for species redistribution. Ecography 40(2):253-266

Lenoir J, Svenning JC (2015) Climate-related range shifts–a global multidimensional synthesis and new research directions. Ecography 38(1):15-28

Lenth R (2019) emmeans: Estimated Marginal Means, aka Least-Squares Means. R package version 1.4.3.01. https://CRAN.R-project.org/package=emmeans

Lieth H (1975) Primary productivity in ecosystems: comparative analysis of global patterns. Unifying concepts in ecology. Springer, pp. 67-88

Lookingbill T, Urban D (2004) An empirical approach towards improved spatial estimates of soil moisture for vegetation analysis. Landscape Ecology 19(4):417-433

Lutz JA, Van Wagtendonk JW, Franklin JF (2010) Climatic water deficit, tree species ranges, and climate change in Yosemite National Park. Journal of Biogeography 37(5):936-950

Major J (1963) A climatic index to vascular plant activity. Ecology 44(3):485-498

Mangiafico S (2020) rcompanion: Functions to Support Extension Education Program Evaluation. R package version 2.3.25.https://CRAN.R-project.org/package=rcompanion

Mather JR (1978) The climatic water budget in environmental analysis. Free Press

Mather JR, Yoshioka GA (1968) The role of climate in the distribution of vegetation. Annals of the Association of American Geographers 58(1):29-41

Maxwell JT, Harley GL, Matheus TJ (2015) Dendroclimatic reconstructions from multiple co-occurring species: a case study from an old-growth deciduous forest in Indiana, USA. International Journal of Climatology 35(6):860-870

McDowell NG, Allen CD (2015) Darcy's law predicts widespread forest mortality under climate warming. Nature Climate Change 5(7):669-672

McDowell RC (1985) The geology of Kentucky. Professional Paper 1151-H, U.S. Geological Survey. http://pubs.usgs.gov/pp/p1151h/

McLaughlin BC, Ackerly DD, Klos PZ, Natali J, Dawson TE, Thompson SE (2017) Hydrologic refugia, plants, and climate change. Global Change Biology 23(8):2941-2961

Meentemeyer V (1978) Macroclimate and lignin control of litter decomposition rates. Ecology 59(3):465-472

Merkle E, You D (2018) nonnest2: Tests of Non-Nested Models. R package version 0.5-2. https://CRAN.R-project.org/package=nonnest2

Millar CI, Westfall RD, Delany DL, King JC, Graumlich LJ (2004) Response of subalpine conifers in the Sierra Nevada, California, USA, to 20th-century warming and decadal climate variability. Arctic, Antarctic, and Alpine Research 36(2):181-200

Miller C, Urban DL (1999) Forest pattern, fire, and climatic change in the Sierra Nevada. Ecosystems 2(1):76-87

Miller W, Miller D (1987) A micro-pipette method for soil mechanical analysis. Communications in soil science and plant analysis 18(1):1-15

Monteith JL Evaporation and environment. In: Symposia of the society for experimental biology, 1965. vol 19. Cambridge University Press (CUP) Cambridge, p. 205-234

Moore ID, Gessler PE, Nielsen GA, Peterson GA (1993) Soil attribute prediction using terrain analysis. Soil Science Society of America Journal 57(2):443-452

Muller RN (1982) Vegetation patterns in the mixed mesophytic forest of eastern Kentucky. Ecology 63(6):1901-1917

Muller RN, McComb WC (1986) Upland forests of the Knobs Region of Kentucky. Bulletin of the Torrey Botanical Club:268-280

Natural Resources Conservation Service, Soil Survey Staff (2019) United States Department of Agriculture. Soil Survey Geographic (SSURGO) Database for Breathitt County, Kentucky. Available online. Accessed January 2020.

Overstreet JC (1984) Robinson Forest inventory. Department of Forestry. University of Kentucky,

Peterson DL, Rolfe GL (1982) Nutrient dynamics and decomposition of litterfall in floodplain and upland forests of central Illinois. Forest Science 28(4):667-681

PRISM Climate Group, Oregon State University, http://prism.oregonstate.edu, created 2019. Accessed January 2020.

R Core Team (2018). R: A language and environment for statistical computing. R Foundation for Statistical Computing, Vienna, Austria. URL https://www.R-project.org/.

Rosenberg NJ, Blad BL, Verma SB (1983) Microclimate: the biological environment. John Wiley & Sons

Rosenzweig ML (1968) Net primary productivity of terrestrial communities: prediction from climatological data. The American Naturalist 102(923):67-74

Seibert J, Stendahl J, Sørensen R (2007) Topographical influences on soil properties in boreal forests. Geoderma 141(1-2):139-148

Seidl R, Thom D, Kautz M et al (2017) Forest disturbances under climate change. Nature climate change 7(6):395-402

Sørensen R, Zinko U, Seibert J (2006) On the calculation of the topographic wetness index: evaluation of different methods based on field observations. Hydrology and Earth System Sciences 10(1):101-112

Stephenson NL (1990) Climatic control of vegetation distribution: The role of the water balance. The American Naturalist 135(5):649-670

Stephenson NL (1998) Actual evapotranspiration and deficit: Biologically meaningful correlates of vegetation distribution across spatial scales. Journal of Biogeography 25(5):855-870

Tarboton DG (1997) A new method for the determination of flow directions and upslope areas in grid digital elevation models. Water resources research 33(2):309-319

Thom AS (1975) Momentum, mass, and heat exchange of plant communities. Vegetation and the Atmosphere 1:57-109

Topp G, Galganov Y, Ball B, Carter M (1993) Soil water desorption curves. Soil sampling and methods of analysis:569-579

Turc L (1961) Estimation of irrigation water requirements, potential evapotranspiration: a simple climatic formula evolved up to date. Ann. Agron 12(1):13-49

VanDerWal J, Murphy HT, Kutt AS et al (2013) Focus on poleward shifts in species' distribution underestimates the fingerprint of climate change. Nature Climate Change 3(3):239-243

Venables WN, Ripley BD (2002) Modern Applied Statistics with S. Fourth Edition. Springer, New York. ISBN 0-387-95457-0

Western AW, Grayson RB, Blöschl G, Willgoose GR, McMahon TA (1999) Observed spatial organization of soil moisture and its relation to terrain indices. Water resources research 35(3):797-810

Whittaker RH (1956) Vegetation of the Great Smoky Mountains. Ecological Monographs 26(1):2-80

Whittaker RH (1966) Forest dimensions and production in the Great Smoky Mountains. Ecology 47(1):103-121

Whittaker RH (1967) Gradient analysis of vegetation. Biological Reviews 42(2):207-264

Whittaker RH, Likens GE (1975) The biosphere and man. Primary productivity of the biosphere. Springer, pp. 305-328

Williamson TN, Agouridis CT, Barton CD, Villines JA, Lant JG (2015) Classification of Ephemeral, Intermittent, and Perennial Stream Reaches Using a TOPMODEL-Based Approach. JAWRA Journal of the American Water Resources Association 51(6):1739-1759

Yeakley JA, Swank W, Swift L, Hornberger G, Shugart H (1998) Soil moisture gradients and controls on a southern Appalachian hillslope from drought through recharge.

Zeileis A, Hothorn T (2002) Diagnostic Checking in Regression Relationships. R News 2(3), 7-10. URL: https://CRAN.R-project.org/doc/Rnews/

Zhu K, Woodall CW, Clark JS (2012) Failure to migrate: lack of tree range expansion in response to climate change. Global Change Biology 18(3):1042-1052

VITA

Education:
Western Kentucky University, Bachelor of Science in Geography and Environmental Studies, Minor in GIS, 2017

Professional Experiences:
University of Kentucky, Graduate Teaching Assistant, 2019- present
University of Kentucky, Gradate Research Assistant, 2018- 2019
Betty Ford Alpine Gardens, Horticultural and Curatorial Intern, 2018
Mount Auburn Cemetery, Plant Records Intern, 2017
Pittsburgh Botanic Garden, Plant Collections Intern, 2017
Bernheim Arboretum and Research Forest, Horticulture Intern, 2016

Honors:
UK Forestry and Natural Resource Sciences Graduate Student Award of Excellence
UK Appalachian Center Eller & Billings Student Research Award
UK Department of Forestry and Natural Resources Graduate Student Conference Award

Katherine J. Love